

Serum Lipocalin-2 (LCN-2) as a major
acute phase protein under different pathological
conditions: *in vivo* and *in vitro* studies

Dissertation
Zur Erlangung des Doktorgrades
der Mathematischen und Natur Wissenschaftlichen Fakultäten
der Georg-August-Universität zu Göttingen

Vorgelegt von
Sadaf Sultan
aus Lahore, Pakistan

Göttingen 2011

D7

Referent: Prof. Dr. Nils Brose

Koreferent: PD Dr. Michael Hoppert

Tag der mündlichen Prüfung: 19.01.2012

Table of Contents

SUMMARY:	1
1. INTRODUCTION	4
1.1 Lipocalin Family.....	4
1.2 Lipocalin-2 (LCN-2)	Fehler! Textmarke nicht definiert.
1.3 Acute Phase response	6
1.4 Acute phase response and Lipocalin-2.....	7
1.5 Radiation induced oxidative stress	7
1.6 Oxidative stress and Lipocalin-2.....	9
1.7 Aim of the study.....	11
2. MATERIALS	12
2.1 Animals.....	12
2.2 Chemicals.....	12
2.3 Other materials.....	15
2.4 Instruments used	15
3. METHODS	18
3.1 Tissue damage and induction of Acute-phase-response.....	18
3.2 Whole rat liver irradiation <i>in vivo</i>	18
3.3 Whole rat lung irradiation <i>in vivo</i>	19
3.4 Blood samples and serum collection	20
3.5 Isolation of rat hepatocytes and irradiation	21
3.5.1 Liver perfusion	21

3.5.2 Preparation of the hepatocyte suspension	21
3.5.3 Media and solutions for hepatocyte preparation and culture	22
3.6 Isolation of rat liver myofibroblasts (liver non-parenchymal cells).....	23
3.6.1 Liver perfusion and preparation of cell suspension.....	24
3.6.2 Separation of nonparenchymal liver cells	24
3.6.3 Purification of myofibroblast by counterflow elutriation.....	25
3.6.4 Media and solutions for myofibroblasts preparation and culture.....	25
3.7 Isolation of rat liver Kupffer cells.....	26
3.8 Real-time polymerase chain reaction	27
3.8.1 RNA isolation for real-time-PCR analysis	27
3.8.1a RNA isolation procedure using silica columns	27
3.8.1b Isolation of RNA by density-gradient ultracentrifugation.....	27
Cell lysis:	27
Homogenization of the tissue sample:.....	27
CsCl gradient and ultra centrifugation:	28
RNA precipitation:	28
Reconstitution of RNA:.....	28
3.8.2 cDNA preparation by reverse transcription	29
3.8.3 Thermal cycler amplification program.....	31
3.8.4 Primer designing.....	31
3.8.5 Statistical analysis	32
3.9 Biochemical methods	32

3.9.1 Protein extraction from liver tissue and cultured hepatocytes.....	32
Preparation of tissue and cell lysates	32
3.9.2 Western blot analysis	33
Sample preparation	33
SDS-polyacrylamide gel	34
SDS-polyacrylamide gel electrophoresis (SDS-PAGE) and electrophoretic transfer	34
Immunovisualization.....	35
3.10 Immunofluorescence Staining	36
3.11 Enzyme-Linked Immunosorbent Assay (ELISA).....	37
3.11.1 Reagent preparation.....	37
3.11.2 Assay Procedure	37
3.12 Safety Measures.....	38
4. RESULTS.....	40
4.1 TO-induced Acute-phase-response.....	40
4.1.1 Serum LCN-2 concentration after TO injection in rat	40
4.1.2 Changes in LCN-2 mRNA in liver from rats treated with turpentine oil: Fehler! Textmarke nicht definiert.	
4.1.3 Changes in α 2M and HO-1 mRNA in liver from TO-treated rats.....	41
4.1.4 Changes in LCN-2 mRNA in kidney and other organs from TO-treated rats	43
4.1.5 Changes in LCN-2 tissue protein in liver from TO-treated rats	44
4.1.6 Changes in LCN2 m-RNA in livers of TO-treated wild type and KO mice as compared to SAA	45

4.1.7 Changes in IL-6, IL-1 β and TNF- α expression in injured TO-treated rat muscle	46
4.1.8 Changes in LCN-2 m-RNA and protein in cytokine-treated rat hepatocytes	Fehler! Textmarke nicht definiert.
4.2 Irradiation induced Liver damage	52
4.2.1 Serum Lipocalin-2 concentration after liver irradiation.....	52
4.2.2 LCN-2 Immunostaining in irradiated liver tissue	53
4.2.3 Real-time PCR analysis of total RNA from rat liver.....	54
4.2.4 Western Blot analysis of rat liver proteins.....	55
4.2.5 Real-time PCR analysis of rat irradiated hepatocytes, myofibroblasts and Kupffer cells.....	56
4.2.6 Real-time PCR analysis of Rat irradiated hepatocytes treated with different cytokines	57
4.3 Irradiation induced Lung damage	59
4.3.1 Serum Lipocalin-2 concentration after lung irradiation.....	59
4.3.2 LCN-2 Immunostaining in irradiated lung tissue	59
4.3.3 Real-time PCR analysis of total RNA from rat lung	60
4.3.4 Real-time PCR analysis of total RNA from liver tissue of lung irradiated experiment.....	60
4.3.5 Western Blot analysis of rat lung proteins	Fehler! Textmarke nicht definiert.
5. DISCUSSION	64
6. REFERENCES	72
7. ACKNOWLEDGMENTS	81
8. DEDICATION	82
9. LIST OF PUBLICATIONS.....	83

10. LIST OF ABSTRACTS	84
11. CURRICULUM VITAE (CV).....	86

List of Figures

Figure 1: Lipocalin-2 family well conserved structure; 3 dimensional, eight stranded antiparallel beta-barrel with a repeated +1 topology enclosing an internal ligand binding site (Chiu et al., 2010).....	5
Figure 2: Schematic diagram: a general overview of acute-phase-response.	6
Figure 3: Free radicals called as reactive oxygen species (ROS) containing unpaired electrons are produced after irradiation which are chemically very active and in turn cause DNA damage and an oxidative stress (adapted by Shikazono et al., 2006).....	8
Figure 4: Computed tomography (CT) scan and dose distribution of rat liver. The marked area was irradiated by AP/PA technique.....	19
Figure 5: Computed tomography (CT) scan and dose distribution of rat lung. The marked area was irradiated by AP/PA technique.....	20
Figure 6: Changes in LCN-2 serum level during APR determined by ELISA. Results are shown in fold \pm standard error of mean (SEM) (* $P \leq 0.05$ analyzed by Student's t-test, n=3).....	41
Figure 7: Changes in gene expression of LCN-2, α 2M and HO-1 mRNA in liver tissue of TO-injected rats determined by Real Time Polymerase Chain Reaction (PCR) analysis. The results were normalized to the housekeeping gene, i.e. beta actin, fold change expression was calculated using threshold cycle (Ct) values and experimental errors are shown as \pm SEM (* $p \leq 0.05$, ** $p \leq 0.005$, *** $p \leq 0.0005$ analyzed by Student's t-test, n = 4).	42
Figure 8: Western blot analysis of LCN-2 (25 kDa), α 2M (168 kDa) and HO-1 (32 kDa) from total protein of TO-treated rat liver. β -actin (42 kDa) was used as loading control.....	45
Figure 9: Changes in gene expression of (a) LCN-2 and (b) SAA in wild type and IL-6 knock-out mice. The results were normalized to the housekeeping	

gene, i.e. GAPDH, and shown in fold \pm SEM (* p \leq 0.05, ** p \leq 0.005, ***p \leq 0.0005 analyzed by Student's t-test, n=3) 47

Figure 10: Changes in gene expression of IL-6, IL-1 β and TNF- α in injured TO-injected rat muscle. The results were normalized to the housekeeping gene, i.e. β -actin and shown in fold \pm SEM (* p \leq 0.05, ** p \leq 0.005, ***p \leq 0.0005 analyzed by Student's t-test, n=3). 48

Figure 11: Changes in gene expression of IL-6, IL-1 β and TNF- α treated hepatocytes. The results were normalized to the housekeeping gene, i.e. β -actin and shown in fold \pm SEM (* p \leq 0.05, ** p \leq 0.005, ***p \leq 0.0005 analyzed by Student's t-test, n=3). 48

Figure 12: Western blot analysis of IL-6-, IL-1 β - and TNF- α -treated hepatocytes with LCN-2 at 6, 12 and 24h along with control. Densitometric analysis of Western blots was also performed to show the changes in protein expression of LCN-2. Results are shown in fold \pm SEM (* p \leq 0.05, ** p \leq 0.005, ***p \leq 0.0005 analyzed by Student's t-test, n=3). 50

Figure 13: Changes in LCN-2 serum level during irradiation determined by ELISA. Results of ELISA are shown in μ g/ml \pm standard error of mean (SEM) (*P \leq 0.05, (**P \leq 0.005 analyzed by Student's t-test, n=3). 53

Figure 14: Changes in LCN-2 serum level during irradiation determined by ELISA Western blot analysis. (LCN-2 25kDa with loading control)..... 53

Figure 15: Immunofluorescence detection of Lipocalin-2 positivity in liver of normal sham irradiated control rats, 1, 6 and 24 hours after irradiation. Sections were stained with an antibody against neutrophil gelatinase associated Lipocalin-2 followed by fluorescence immunodetection (original magnification 200x). 54

Figure 16: Fold changes of mRNA expression of Lipocalin-2 in irradiated liver tissue at time points from 1 hour to 48 hours related to normal sham irradiated control rats determined by Real Time Polymerase Chain Reaction (PCR). The results were normalized to the housekeeping gene, i.e. β -actin, fold change expression was calculated using threshold cycle (CT) values and experimental

errors are shown as \pm SEM (* p \leq 0.05, ** p \leq 0.005, ***p \leq 0.0005 analyzed by Student's t-test, n = 3). 55

Figure 17: Western blot analysis of LCN-2 (25 kDa) from total protein of different timepoints from irradiated liver including normal sham irradiated animals. Beta actin (42 kDa) was used as loading control. 56

Figure 18: Fold changes of mRNA expression of LCN-2 in different irradiated liver cells (hepatocytes, myofibroblasts and kupffer cells) at different time points related to normal sham irradiated control cells determined by real time polymerase chain reaction (PCR). The results were normalized to the housekeeping gene, i.e. beta actin, fold change expression was calculated using threshold cycle (Ct) values and experimental errors are shown as \pm SEM (* p \leq 0.05, ** p \leq 0.005, ***p \leq 0.0005 analyzed by Student's t-test, n = 3). 57

Figure 19: Fold changes of mRNA expression of LCN-2 in IL-6-, IL-1 β -, TNF- α - and IL-6+TNF- α -treated hepatocytes. The results were normalized to the housekeeping gene, i.e. β -actin, and are shown as \pm SEM (* p \leq 0.05, ** p \leq 0.005, ***p \leq 0.0005 analyzed by Student's t-test, n = 3). 58

Figure 20: Double Immunofluorescence detection of Lipocalin-2 and Myeloperoxidase positive cells in lung sections of normal sham irradiated control rats, 1, 6 and 24 hours after irradiation. Sections were stained with an antibody against Lipocalin-2 and Myeloperoxidase followed by double fluorescence immunodetection. 60

Figure 21: Fold changes of mRNA expression of Lipocalin-2 in irradiated lung tissue at time points from 1 hour to 48 hours related to normal sham irradiated control rats determined by Real Time Polymerase Chain Reaction (PCR). The results were normalized to the housekeeping gene, i.e. β -actin, fold change expression was calculated using threshold cycle (CT) values and experimental errors are shown as \pm SEM (* p \leq 0.05, ** p \leq 0.005, ***p \leq 0.0005 analyzed by Student's t-test, n = 3). 61

Figure 22: Fold changes of mRNA expression of LCN-2 in upper and lower liver of lung irradiated rats at different time points related to normal sham irradiated

control rats determined by real time polymerase chain reaction (PCR). The results were normalized to the housekeeping gene, i.e. beta actin, fold change expression was calculated using threshold cycle (Ct) values and experimental errors are shown as \pm SEM (* p \leq 0.05, ** p \leq 0.005, ***p \leq 0.0005 analyzed by Student's t-test, n = 3).	62
Figure 23: Western blot analysis of LCN-2 (25 kDa) from total protein of different timepoints from irradiated lung including normal sham irradiated animals. Beta actin (42 kDa) was used as loading control.	63
Figure 24: Homeostasis disturbance in body cause release of different cytokines, these cytokines induce Lipocalin-2 production in liver. This Lipocalin-2 via blood triggers leukocytosis and healing.	64
Figure 25: Difference between Cycle threshold (Ct) values of Liver tissue and IL-6 treated hepatocytes at same time points.....	66
Figure 26: A pathway showing Lipocalin-2 activation, secretion and then mode of action in a damage model of liver irradiation.	68
Figure 27: A pathway showing Lipocalin-2 activation, secretion and then mode of action in a damage model of lung irradiation.	69

List of Tables

Table 1: Primer sequences used for real-time PCR analysis

Table 2: Changes in LCN2 gene expression in liver, kidney, heart, brain, spleen and lung. Results are shown in fold \pm SEM (n=3).

Table 3: Threshold cycle (Ct) values of RT-PCR analysis of LCN-2, α 2M and HO-1 in total liver tissue (upper part) and IL-6 treated hepatocytes (lower part) mRNA (Ctmean \pm SEM) (n=3).

Abbreviations

α 2M α 2-macroglobulin

Ab Antibody

APP Acute phase proteins

APR Acute phase response

BSA Bovine serum albumin

BV Biliverdin

BV-R Biliverdin reductase

cAMP Cyclic adenosine-3',5'-monophosphate

cDNA Copy deoxyribonucleic acid

cGMP Cyclic guanosine monophosphate

C/EBP Ccaat-enhancer-binding proteins

CO Carbon monoxide

CREB cAMP response element-binding protein

CRP C-reactive protein

CT Threshold cycle

dd H₂O Double distilled water

DEPC Diethylpyrocarbonate

DMSO Dimethylsulfoxide

DNA de-ribonucleic acid

dNTP Deoxyribonucleoside triphosphate

DTT Dithiothreitol

EDTA Ethylenediaminetetraacetic acid

ELISA Enzyme-linked immunosorbent assay

Fluorescence

FCS Fetal calf serum

g Gram

GAPDH Glyceraldehyde-3-phosphate dehydrogenase

GFP Green fluorescent protein

gp Glycoprotein

Gy Gray

h hour

HO-1 Hemoxygenase-1

HEPES 2-(4-2-hydroxyethyl)-piperazinyl-1-ethansulfonate

HPLC High performance liquid chromatography

IgG Immunoglobulin G

IL Interleukin

IP Intraperitoneal

Kb Kilobase

kDa Kilodalton

kg Kilo-gram

KO Knock-out

LCN-2 Lipocalin-2

LPS Lipopolysaccharide

mRNA Messenger Ribonucleic acid

MV mega-volt

NIH National institute of health

NGAL Neutrophil gelatinase associated lipocalin

NF- κ B Nuclear factor κ B

OD Optical density

PBS Phosphate buffered saline

PCR Polymerase chain reaction

PMSF Phenylmethyl sulfonylfluoride
RILD Radiation-induced liver disease
RNase Ribonuclease
ROS Reactive oxygen species
rpm Rounds per minute
RT Radiation therapy
RT Room temperature
RT-PCR Reverse transcriptase-PCR
SAA Serum-amyloid-A
SDS Sodium dodecylsulfate
SDS-PAGE SDS-polyacrylamide gel electrophoresis
SEM Standard error of the mean
TEMED N, N, N', N'-tetramethylethylenediamine
TO Turpentine oil
TNF- α Tumor necrosis factor α
Tris Tris-(hydroxymethyl)-aminomethane
U Unit
UBC Ubiquitin C
UV Ultraviolet
WB Western blot
WT wild type

SUMMARY:

Lipocalin-2 (LCN-2) is a pleiotropic 25-kDa secretory protein, currently used as a biomarker for renal injury and inflammation. Its serum level is increased under different pathological conditions but the source and cause are unclear. The aim of our study was to prospectively evaluate the LCN-2 expression in different pathological conditions.

The objective of our study was to determine LCN-2 expression in a rat and mouse model of sterile abscess and in a model of rat liver and lung exposed to single dose x-irradiation as oxidative stress is induced in both models.

The current study compares LCN-2 gene expression with known major acute phase proteins in the liver in a rat and mouse model of turpentine-oil (TO)-induced sterile abscess. Furthermore, it shows that serum Lipocalin-2 is a potential Biomarker of radiation damage of liver but not lung.

Serum LCN-2 concentrations increased dramatically up to 200-fold (20 µg/ml) at 48h after TO-injection. A strong elevation of LCN-2 mRNA in rat liver was observed starting from 4h up to 48h after injection, with a maximum (8738 ± 2104 -fold) at 24h, which was further confirmed by Western blot analysis. In contrast, the increases in gene expression of α 2-macroglobulin (α 2M), the major acute phase protein and hemoxygenase-1 (HO-1), a positive acute phase protein were only 1025 ± 505 and 47 ± 12 -fold respectively during acute-phase-response. No considerable change was observed in LCN-2 mRNA in rat kidney and other organs as compared to liver.

Using the IL-6 knockout mice model, wild type mice showed a strong LCN-2 expression, with a maximum of 2498 ± 84 -fold in the liver, which is similar to that for serum-amyloid-A (SAA) (2825 ± 233 -fold), a major mouse acute phase protein. However such an increase was significantly inhibited in IL-6^{ko} mice during APR. IL-6 treated rat hepatocytes induced a significant time dependent up-regulation of LCN-2, indicating that LCN-2 is active on the executive side of the acute phase response, which is induced by IL-6.

Also in our second model of acute phase reaction, LCN-2 serum levels increased significantly (up to 2.5 fold) within 24 hours after direct liver irradiation. No increase in serum levels were detected lung irradiation. LCN-2 specific transcripts increased significantly up to 552 ± 109 -fold at 24h after liver irradiation which was further confirmed by western blot analysis. Immunohistology of the liver detected positivity in recruited granulocytes within 1 hour after irradiation around central and portal fields.

LCN-2 mRNA level of lung tissue showed an increased expression at 24 hours (9 ± 2.3 -fold) which was further confirmed at protein level by Western blot analysis. Lung immunohistology showed a high constitutive expression due to the high number of granulocytes.

Irradiated hepatocytes showed higher LCN-2 expression as compared to myofibroblasts and Kupffer cells. Cytokine treatment specially IL-1 β further increased LCN-2 gene expression in cultured hepatocytes.

The current study compares LCN2 gene expression with known major acute phase proteins in the liver in a rat and mouse model of turpentine-oil (TO)-induced sterile abscess. LCN-2 is the major acute-phase protein as compared to α 2M and HO-1 in rat and comparable with SAA in mouse. The gene

expression is mainly controlled by IL-6. The liver is the main source of serum LCN-2 in the case of different acute-phase-responses supporting our earlier finding, the hepatocytes and not the granulocytes are the source for LCN-2 production in the liver and increased serum levels of LCN-2 in acute-phase-response.

Single dose liver irradiation, but not lung irradiation induces a fast and significant increase of LCN-2 serum level. LCN-2 may be a suitable biomarker not only in acute-phase-response induced in TO model but also to determine the irradiated liver volume retrospectively in case of accidental liver irradiation to avoid RILD.

1. INTRODUCTION

1.1 Lipocalin Family

Lipocalin family is the member of superfamily calycin and includes over 20 small, mostly soluble, secretory proteins with three well conserved motifs (20% identity). Their three-dimensional structure, in fact, comprises a single eight-stranded, continuously hydrogen-bonded antiparallel β -barrel, that forms an enclosing cavity, thought to be able to bind a wide variety of small molecules, such as retinoids, arachidonic acid, steroids and iron (Flower, 1996).

It is thought to be involved in the induction of apoptosis (Devireddy et al., 2001), the transport of fatty acids and iron, the suppression of bacterial growth, and to act as an antagonist of inflammatory molecules and the modulation of cellular processes by binding to the ligands and interacting with the specific cell surface receptors (Flower, 1996; Yang et al., 2002). The lipocalin family in general plays the role of transporters with several different functions, including regulation of immune responses, modulation of cell growth and metabolism, iron transportation and prostaglandin synthesis (Yang et al., 2002).

1.2 Lipocalin-2 (LCN-2)

Lipocalin-2 is a secretory protein and exists as a 25kDa monomer and 46kDa homodimer. The primary LCN-2 transcript is 3.696 nucleotides long and the processed transcript is 809 nucleotides long. It is known as neutrophil gelatinase associated lipocalin because it was first identified as a matrix protein of specific granules of human neutrophils (Kjeldsen et al., 1994). LCN-2 has also been shown to be a bacteriostatic agent capable of binding iron in the form

of siderophores by a non-heme compound which consequently sequesters it from inflammation and infection sites (Berger et al., 2006; Flo et al., 2004).

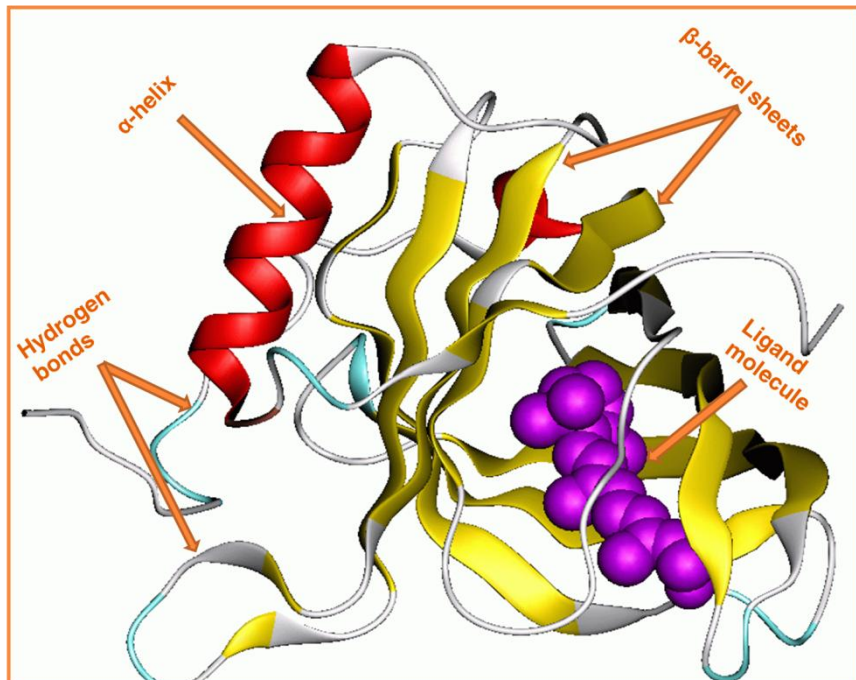


Figure 1: Lipocalin-2 family well conserved structure; 3 dimensional, eight stranded antiparallel beta-barrel with a repeated +1 topology enclosing an internal ligand binding site (Chiu et al., 2010).

It is also called uterocalin as LCN-2 appears to be expressed at high levels in epithelial cells of the uterus during pregnancy and suggested as a part of local inflammatory response during parturition (Liu et al., 1997). Promoter regions of both LCN-2 and its murine homolog 24p3 have been found to contain consensus sequences for several different transcription factors, including NF- κ B, C/EBP and CREB (Cowland et al., 2006; Cowland et al., 2003; Shen et al., 2006). So far, cytokine-mediated LCN-2 expression patterns are not yet completely clear, and some of our studies provide inconclusive data (Ramadori et al., 1985; Tron et al., 2005).

1.3 Acute Phase response

The acute-phase-response (APR) is the defense reaction of an organism against infectious and harmful agents that attack its integrity. This reaction is aimed to restrict the area of damage on one side and to eliminate, or at least isolate the harmful element on the other side. In acute-phase-response inflammatory cells infiltrate the first line of defense against any pathogen, i.e. noxae or traumatic tissue injury produces an abundance of soluble mediators and the increase in their concentrations in serum.

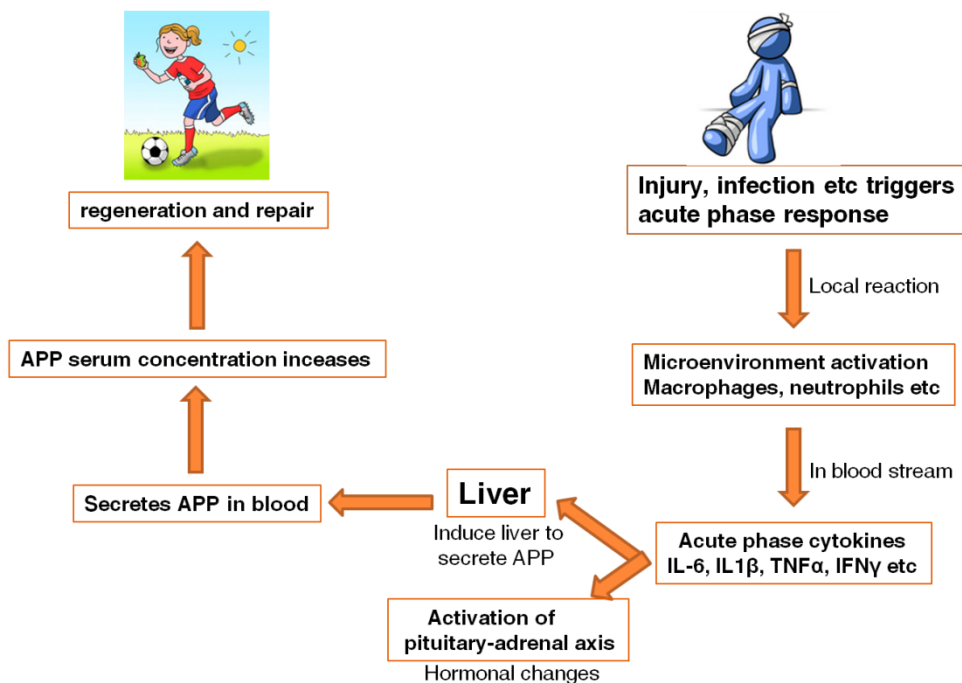


Figure 2: Schematic diagram: a general overview of acute-phase-response.

Acute-phase-cytokines are responsible for more generalized symptoms of the APR, such as fever, malaise and somnolence, loss of appetite, muscular pain, hyperglycemia and hypoferaemia. IL-6 is the main acute phase mediator (Papanicolaou et al., 1998; Ramadori et al., 2010) due to the changes in *de novo* synthesis and secretion of positive acute phase proteins alongside with a

decreased production of negative acute phase proteins such as albumin. The purpose of these metabolic and systemic changes is to control the defense mechanisms, maintain vital body functions during inflammation and eventually to restore body homeostasis (Moshage, 1997).

1.4 Acute phase response and Lipocalin-2

The major acute phase protein in humans is C-reactive protein (CRP) (Pepys and Hirschfield, 2003), its serum levels having been shown to increase by up to a 1000-fold during APR. In the rat this role is played by α 2M (Kushner, 1993) and in the mouse by SAA (Ramadori et al., 1985). The role of LCN-2 under APR has not been studied specifically at serum level so far. Other studies show that an increase of LCN-2 serum concentrations can be detected in various inflammatory conditions of the intestinal tract such as appendicitis, inflammatory bowel disease and diverticulitis (Alpizar-Alpizar et al., 2009; Sunil et al., 2007), and systemic inflammatory states such as sepsis. Urine and serum LCN-2 concentrations increased after ischemia/reperfusion injury of the kidney, and urine LCN-2 concentration was inversely proportional to the creatinine serum level. It was concluded that increased serum and urine LCN-2 levels were due to increased kidney production (Mori et al., 2005).

1.5 Radiation induced oxidative stress

Radiation therapy involves the use of high energy rays to treat local or regional malignancies either alone or with other modalities e.g. chemotherapy or surgery. Free radicals such as reactive oxygen species (ROS) containing unpaired electrons are generated after irradiation in irradiated tissue (Riley,

1994) and cells which are chemically very active are prone to oxidative stress (Winterbourn, 2008). Many physiological and cellular processes are effected by oxidative stress such as gene expression, cell growth and cell death (Esmekaya et al., 2011). Radiation is also known to induce DNA damage and chromosomal instability of cells both from tumorous and normal tissue (Sakata et al., 2007). There are further mechanisms involved in the actions occurring after the exposure of cells and tissue due to ionizing radiation, such as radiation-induced-apoptosis (Hasegawa et al., 2002).

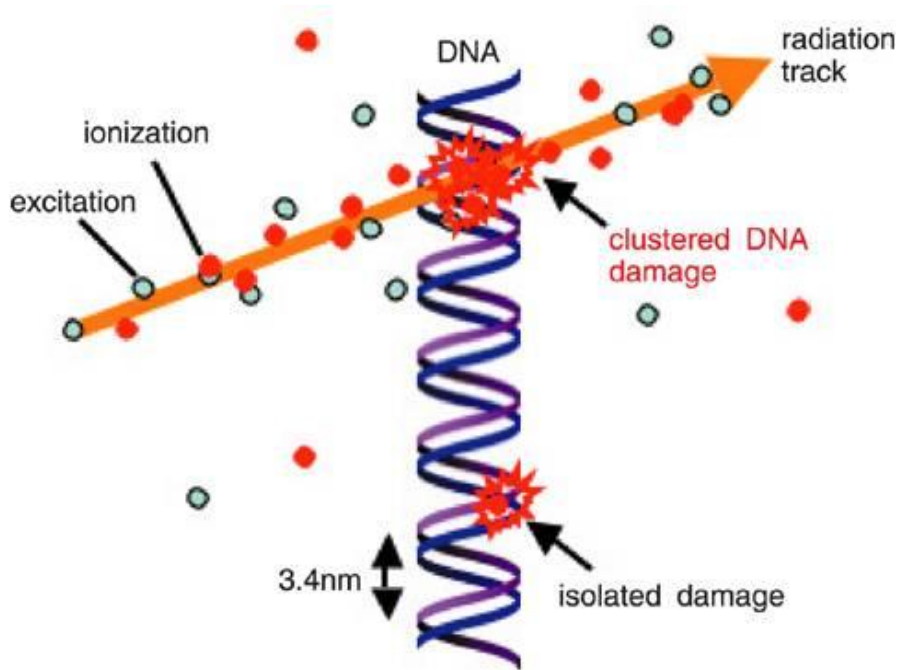


Figure 3: Free radicals called reactive oxygen species (ROS) containing unpaired electrons are produced after irradiation which are chemically very active and in turn cause DNA damage and an oxidative stress (Shikazono et al., 2006).

Therapeutic radiation causes both acute and chronic toxicity in normal tissue (Citrin et al., 2010). Furthermore, due to increase utilization of nuclear technologies in industries and hospitals, the risk of accidental radiation

exposure increase to workers, patients and radiologists (Pandey et al., 2010). In these cases, certain biomarkers are suitable to retrospectively evaluate radiation exposure, e.g. the number of blood cells, the frequency of chromosomal aberrations in the blood cells, and the amount of radiosensitive material in urine, (HEUSTIS and FAROWE, 1951).

Lung cancers are frequently treated with radiotherapy with the advent of respiratory gated radiotherapy and the amelioration of stereotactic techniques, radiotherapeutic interventions at the liver gain increasing interest, especially for the treatment of liver tumors or metastases (Berbeco et al., 2005; Schefter et al., 2005).

1.6 Oxidative stress and Lipocalin-2

Increased Lipocalin-2 gene expression has been shown in oxidative stress induced by chemicals such as diethylnitrosamine which is a major producer of ROS (Lechner et al., 2001; Meyer et al., 2003). Several studies have reported the Lipocalin-2 expression under stress conditions caused by free radicals such as inflammation, toxicity, chronic kidney disease; myocardial infarction and burn injury, infections and several types of cancers (Hemdal et al., 2006; Mishra et al., 2006; Mishra et al., 2004; Missiaglia et al., 2004; Nielsen et al., 1996; Vemula et al., 2004; Viau et al., 2010).

In the absence of cellular stress, LCN-2 maintained a low steady-state level and exerts very little, if any effect on the fate of tissue (Sultan et al, 2011) (Flower, 1994). Lipocalin-2 serum levels are increased under several conditions. We recently showed that Lipocalin-2 is a major acute phase protein in the rat and its

gene expression is regulated by IL-6 and IL-1 β in hepatocytes (Sultan et al, 2011).

1.7 AIM OF THE STUDY

The first aim of this study was to analyze the kinetics of LCN-2 serum levels together with gene and protein expression in rat liver in comparison to the other parenchymal organs, presently considered a major producer of LCN-2 in several pathological conditions. We established that LCN-2 is a much stronger positive acute phase protein than the major acute phase proteins α 2M and positive acute phase protein HO-1 (Tron et al., 2005) in rats and comparable with SAA in mice. The main source is most probably the liver and the up-regulation is mostly regulated by interleukin-6 (IL-6).

The second aim was to analyze the kinetics of Lipocalin-2 serum levels in addition to evaluate the Lipocalin-2 gene and protein expression in rat liver exposed to single dose of x-irradiation. Furthermore, immunofluorescence staining was also performed to show Lipocalin-2 localization within the damaged tissue. Lipocalin-2 expression was further shown in isolated liver cells, irradiated and treated with cytokines, such as TNF- α , IL-6, and IL-1 β to determine the effect of different cytokines on Lipocalin-2 production.

Furthermore, we determine whether only liver irradiation cause an increase in serum LCN-2 expression. To prove this hypothesis we irradiated the lung and evaluated the LCN-2 gene and protein expression in addition to immunofluorescence staining.

Notably, in the lung irradiation experiment, the upper part of the liver was within the radiation field, because it lay right below the lung. So our fourth objective was to evaluate the LCN-2 expression of the liver when it was not directly irradiated.

2. MATERIALS

2.1 Animals

Male Wistar rats of about 170-200 g body weight were purchased from Harlan Winkelmann (Brochen, Germany). Male WT C57Black6 mice were purchased from Harlan-Winkelmann Germany and IL-6 KO mice (B6.129S2-IL6tm1Kopf/J) were purchased from Jackson Laboratories USA. All animals were 8 weeks of age. The animals were kept under standard pathogen free conditions with 12 h light/dark cycles and *ad libitum* access to fresh water and food pellets. Approximately 12-15g food and 12-25 ml Water was consumed by each rat and they gained approx. 30-40g of weight per week. All animals were cared for according to the institutional guidelines, the German convention for the protection of animals and NIH guidelines.

2.2 Chemicals

All chemicals were of analytical grade and obtained from commercial sources as indicating follow

- Amersham pharmacia Biotech /Freiburg, Germany**

α -₃₂P-labelled deoxy-cytidine-triphosphate (specific activity 3000 Ci/mmol)

- Biochrom /Berlin, Germany**

M199

FCS (fetal calf serum)

Trypan blue

- **Bioline /Luckenwalde, Germany**

dNTP mastermix

- **Bio-Rad /Munich, Germany**

Tween 20

- **Bohringer /Mannheim, Germany**

Ampicillin

- **Fresenius / Bad Homburg, Germany**

Ampuwa water

- **Invitrogen /Karlsruhe, Germany**

Guanidine isothiocyanate

Trizol reagent

- **Merck /Darmstadt, Germany**

Acetic acid glacial

Acetone

Bromophenol blue

Carbon tetra chloride

Ethanol

37% formaldehyde

Formamide

Glucose

Glycerol

Kaiser' s gelatine

Meyer' hemalaun

Methanol

β - mercaptoethanol

Penicillin G

Streptomycin

TEMED

- **Merial /Hallbergmoos, Germany**

Pentobarbital sodium (NarcorenR)

- **PAA /Linz, Austria**

L-Glutamine

- **Paesel and Lorei /Frankfurt, Germany**

Cesium chloride

- **Roth /Karlsruhe, Germany**

Glycine

Sodium dodecyl sulfate (SDS)

- **Serva /Heidelberg, Germany**

Tris HCl

- **Sigma-Aldrich Chemie /Munich, Germany**

Ammonium persulfate

Citric acid

Dexamethasone

DMSO

DTT

EDTA

Ethidium bromide

HEPES

Sodium acetate

Sodium citrate

Triton X-100

- **University Apotheke Goettingen /Goettingen, Germany**

Turpentine oil

2.3 Other materials

X-ray films Hyperfilm TM, Amersham Biosciences / Freiburg, Germany

Syringes BD Discardit 2ml, 5ml, 20ml Becton Dickinson /NJ, USA

Sterile filter pipette tips, Biozym / Oldendorf, Germany

Sterile filter Nalgene, 0.2 µm, Sartorius /Göttingen, Germany

Serological pipettes (2, 5, 10, 25ml), transfer pipettes, plastic tubes (15 and 50ml), Sarstedt /Germany

Safe-Lock tubes (0.2, 0.5, 1,5 and 2 ml), Eppendorf /Hamburg, Germany

Braunules 2G14, Braun /Melsungen, Germany

Culture dishes (60 mm) Falcon, Becton Dickinson /NJ, USA

Hybond N nylon membrane, disposable NICK columns prepacked with SephadexR Hybridization glass tubes, Biometra /Goettingen, Germany

2.4 Instruments used

Step One plus Thermal cycler (Applied Biosystems), USA

Clinac 600C; Varian, Palo Alto, Calif

Microscope Axioscop with photo camera MC 100 Spot, Zeiss /Oberkochen, Germany

Microscope Axiovert 25, Zeiss /Oberkochen, Germany

pH-Meter 761 Calimatic, Knick /Berlin, Germany

Power supply, Power Pac 300, Bio-Rad /Munich, Germany

Savant Speed VacR concentrator, ThermoLife Sciences /Egelsbach, Germany

Sterile bench, type Lamin Air, TL 2472, Heraeus /Hanau, Germany

Sterile bench, type MRF 0.612-GS, PrettL Laminarflow and Prozesstechnick /Bempflingen, Germany

Somatom Balance; Siemens Medical Solutions, Erlangen Germany

Thermomixer 5436, Eppendorf /Hamburg, Germany

Thermostat, Heraeus /Hanau, Germany

Ultra-Turrax TP 18/10 homogenizer, jank & Kunkel /Staufen, Germany

Ultraviolet emitter, 312nm, Bachofer /Reutlingen, Germany

UV spectrophotometer, RNA/DNA Calculator GeneQuant II, Pharmacia Biotech /Freiburg, Germany

Vortex, Genie 2TM, Bender and Hobein /Zurich, Switzerland

Vortex with platform, Schutt Lambortechnic /Goettingen, Germany

Water bath 1083, GFL /Burgwedel, Germany

Magnetic mixer with warming, type M21/1 farmo-Geratechnik /Germany

Ice machine, Ziegra /Isernhagen, Germany

Incubator with shaking for cell culture, model 3-25, New Brunswick Scientific Co., Inc. /Edison, New Jersey, USA

Microwave oven, Siemens, Germany

X-ray film cassettes 10x18, Siemens, Germany

X-ray film developing machine SRX-101A, Konica Europe /Hohenbrunn, Germany

Bench-top, high speed and ultracentrifuges

Beckman model J2-21 centrifuge and Backman rotor JE-6B, Bechman /Munich, Germany

Centricon T-2070 ultracentrifuge and Centricon rotor TST55.5-55000rpm Kontron instruments /Neufahrn, Germany

Eppendorf bench-top centrifuge, type MiniSpin 5415C Eppendorf/ Hamburg, Germany

Hettich Mikro Rapid/K centrifuge, 3850 centrifuge, 48RS centrifuge, Hettich Rotaxia/RP centrifuge Hettich /Tuttlingen, Germany

3. METHODS

3.1 Tissue damage and induction of Acute-phase-response

Acute-phase-response was induced in ether-anaesthetized rats by an intramuscular injection of 5ml/kg TO in both the right and the left hind limbs (Tron et al., 2005). Control animals for each time point received a saline injection. The animals were sacrificed at different time points from 0 h to 48 h after TO injection under pentobarbital sodium anaesthesia (Hallbergmoos, Germany). The liver, kidney, heart, lung, brain, spleen and injured muscle were excised and minced, rinsed with physiological sodium saline, snap frozen in liquid nitrogen and stored at -80° C till further use.

Mice were given 10 ml/kg TO i.e., 100µl treated as described above. Animals were sacrificed at different time points from 0h to 24h after treatment and processed further as above.

3.2 Whole rat liver irradiation *in vivo*

We established a rat model of CT-driven single organ x-irradiation as described earlier (1). For *in vivo* experiments, a planning CT scan (Somatom Balance, Siemens, Erlangen, Germany) was done on each intraperitoneally anesthetized rat (90 mg/kg ketamine [Intervet, Unterschleißheim, Germany], 7.5 mg/kg xylazine 2% [Serumwerk Bernburg AG, Bernburg/ Saale, Germany]) to delineate the liver of the animals. The margins of the liver were marked on the skin of the animals, and a dose distribution was calculated. Exemplary dose distributions for liver irradiation are shown in figures 1 and 2, respectively. Irradiation was performed with 6 MV photons (dose rate of 2.4 Gy/min) using a

Varian Clinac 600 C accelerator (Varian, Palo Alto, USA). Thereby, for liver irradiation a single dose of 25 Gy was delivered using an AP/PA treatment technique.

Treated animals and sham-irradiated controls were killed humanely 1, 3, 6, 12, 24 and 48 hours after irradiation. Liver were taken carefully, rinsed with 0.9% 119 NaCl and preserved at -80°C for real time RT-PCR analysis, western blot analysis and cryostat section cutting.

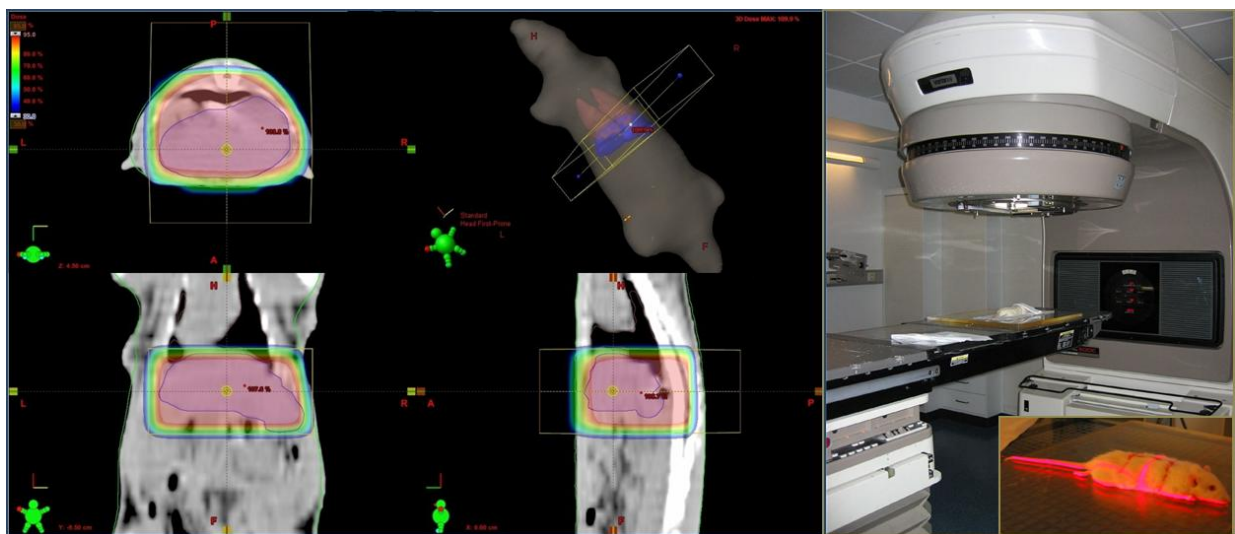


Figure 4: Computed tomography (CT) scan and dose distribution of rat liver. The marked area was irradiated by AP/PA technique (by courtesy of Radiology Department, University Klinikum Göttingen).

3.3 Whole rat lung irradiation *in vivo*

A single dose of 25 Gy was given to animals after planning CT scan as described above for liver irradiation. Lung of the animals was marginate and then irradiate as described above with same technique. Treated animals and sham-irradiated controls were killed humanely 1, 3, 6, 12, 24 and 48 hours after irradiation. Liver were taken carefully, rinsed with 0.9% 119 NaCl and preserved

at -80°C for real time RT-PCR analysis, western blot analysis and cryostat section cutting.

Notably, in the lung irradiation experiment, the upper part of the liver was within the radiation field, because it lay right down to the lung (see figure 2). So the liver tissue was separated as upper liver (within the planned radiation field) and lower liver (outside the planned radiation field) to compare gene expression in both parts of the liver.



Figure 5: Computed tomography (CT) scan and dose distribution of rat lung. The marked area was irradiated by AP/PA technique (by courtesy of Radiology Department, University Klinikum Göttingen).

3.4 Blood samples and serum collection

Blood samples were collected in special serum tubes (Sarstedt Monovette) from the inferior vena cava of the control and treated animals, allowed to clot overnight at 4°C and centrifuged for 20 min at 2000g. Serum was removed and stored at -80°C.

3.5 Isolation of rat hepatocytes and irradiation

Hepatocytes were isolated from male Wistar rats by circulating perfusion with collagenase essentially as described previously (Seglen, 1972).

3.5.1 Liver perfusion

The vena portae was canulated after laparotomy and then vena cava inferior was ligated above the diaphragm to prevent flow of the perfusion media into the whole body circulation. Finally, the vena cava inferior was cut beneath the liver and canulated. The liver was perfused in non-recirculatory mode through the portal vein with 150-200 ml CO₂-enriched preperfusion medium at a flow rate of 30 ml/min until the liver was free from blood. To break down components of extracellular matrix, the liver was perfused in recirculatory mode with collagenase perfusion medium until it started to feel soft (about 7-11 min).

3.5.2 Preparation of the hepatocyte suspension

After perfusion, the liver was excised and transferred into a sterile glass beaker filled with culture medium M 199 with additives. Glisson's capsule, i. e. collagen tissue around the liver, was carefully removed and discarded. To obtain a cell suspension, the tissue was disrupted mechanically using sterile forceps. Connective tissue and remainder of the liver capsule as well as big cell aggregates were removed by filtration of the primary cell suspension through a nylon mesh (pore-size 79 µm). Non-parenchymal cells and cell debris were removed by numerous selective sedimentations (20 g, 2 min, 4°C) in wash medium. After the last centrifugation, hepatocytes were suspended in medium M 199 with additives. 50 ml of M 199 was added per 1 g of wet weight of the

sedimented cells; the cell suspension typically had a density of about 106/2.5 ml.

3.5.3 Media and solutions for hepatocyte preparation and culture

All media and solutions for cell culture were prepared in double distilled water, further purified by sterile filtration and stored at 4°C. All solutions were prepared not more than one day before the isolation.

Krebs-Ringer stock solution

	Final concentration
<u>NaCl</u>	<u>120 mM</u>
<u>KCl</u>	<u>4.8 mM</u>
<u>MgSO₄·7H₂O</u>	<u>1.2 mM</u>
<u>KH₂PO₄</u>	<u>1.2 mM</u>
<u>NaHCO₃</u>	<u>24.4 mM</u>

The solution was equilibrated with carbogen and pH was adjusted to 7.35

Pre-perfusion medium (prepared in 1X Krebs-Ringer solution)

	Final concentration
<u>EGTA</u>	<u>0.25 mM</u>

Collagenase perfusion medium (prepared in 1X Krebs-Ringer solution)

	Final concentration
<u>HEPES</u>	<u>15 mM</u>
<u>CaCl₂·2H₂O</u>	<u>4 mM</u>
<u>Collagenase</u>	<u>50 mg</u>

The medium was prepared directly prior to isolation, equilibrated with carbogen for 30 min and finally sterile filtered.

Wash medium

	Final concentration
<u>HEPES/NaOH pH 7.4</u>	<u>20 mM</u>
<u>NaCl</u>	<u>120 mM</u>
<u>KCl</u>	<u>4.8 mM</u>
<u>MgSO₄·7H₂O</u>	<u>1.2 mM</u>
<u>KH₂PO₄</u>	<u>1.2 mM</u>
<u>Bovine serum albumin</u>	<u>0.4%</u>

Medium M 199 with additives

<u>M199 with Earle's salts without NaHCO₃</u>	<u>Final concentration</u>
<u>Glucose·H₂O</u>	<u>5.5 mM</u>
<u>HEPES</u>	<u>15 mM</u>
<u>NaHCO₃</u>	<u>18 mM</u>
<u>Bovine serum albumin</u>	<u>0.4%</u>

The medium was equilibrated with carbogen until pH reached a value of 7.35.

Finally, the medium was sterile filtered.

3.6 Isolation of rat liver myofibroblasts (liver non-parenchymal cells)

Rat liver myofibroblasts were isolated according to the method previously described (Dudas et al. 2007) with slight modifications.

3.6.1 Liver perfusion and preparation of cell suspension

The laparotomy and canulation were performed essentially as described above.

The liver was perfused with preperfusion medium containing Gey's Balanced Salt Solution (GBSS) and sodium hydrocarbonate, followed by perfusion with enzyme solution 1 containing pronase with subsequent change to enzyme solution 2 containing pronase and collagenase.

After perfusion, the liver was excised and placed into the sterile Petri dish filled with enzyme solution 3 containing pronase, collagenase and DNase I and was mechanically disrupted with sterile forceps. The cell suspension obtained was stirred in the same perfusion solution for 30 min with simultaneous control of pH (7.5) and finally filtered through the sterile sieve and collected in 50 ml polypropylene tubes. To separate big cell aggregates and major part of the parenchymal liver cells, the suspension was centrifuged for 4 min at 35 g (4°C).

The supernatant was re-centrifuged for 5 min at 640 g (4°C), the pellet was resuspended in 50 ml of GBSS containing 100 µl DNase I.

3.6.2 Separation of nonparenchymal liver cells

Nonparenchymal liver cells were separated using Nycodenz® density gradient as follows: the cell suspension was transferred into four sterile 50 ml polypropylene tubes and centrifuged for 5 min at 640 g (4°C). The supernatant was discarded and the pellets were resuspended in a small volume (5-6 ml) of GBSS with 100 µl DNase I and pooled together in one sterile 50 ml polypropylene tube. 14 ml of 30% Nycodenz was added and the volume was adjusted to 24 ml with GBSS. This mixture was divided between four sterile 15 ml polypropylene tubes and GBSS (1.5 ml per tube) was carefully layered over

the content of the tubes. The gradient was centrifuged for 15 min at 1,800 g (4°C). Afterwards, the interphase brown layer between Nycodenz and GBSS containing nonparenchymal liver cells was carefully transferred into sterile 50 ml polypropylene tube and centrifuged for 5 min at 640 g (4°C).

3.6.3 Purification of myofibroblast by counterflow elutriation

To obtain pure of myofibroblast, nonparenchymal liver cells were fractionated by centrifugal counterflow elutriation according to (Knook and Sleyster 1976). The nonparenchymal liver cell pellet obtained in the previous step was resuspended in 5-6 ml of 0.4% BSA/GBSS, collected in a sterile 10 ml syringe and injected in the elutriation system. Using a JE-6B elutriation rotor assembled according to the manufacturer's instructions and spun at 2,500 rpm in a J2-21 centrifuge (Beckman Instruments), fractions enriched with sinusoidal endothelial cells, myofibroblasts and Kupffer cells were collected at flow rates of 19 ml/min, 23 ml/min and 55 ml/min, respectively. The myofibroblast fractions were sedimented by centrifugation (5 min at 640 g, 4°C), counted in a Neubauer chamber and, after assessment of cell viability by Trypan blue staining, taken up in a culture medium.

3.6.4 Media and solutions for myofibroblasts preparation and culture

All media and solutions for cell culture were prepared in double distilled water, further purified by sterile filtration and stored at 4°C, unless otherwise indicated.

10X GBSS (Gey's Balanced Salt Solution)

<u>NaCl</u>	<u>80g</u>
<u>KCl</u>	<u>3.7g</u>
<u>MgSO₄·7H₂O</u>	<u>0.7g</u>
<u>NaH₂PO₄·H₂O</u>	<u>1.7g</u>
<u>CaCl₂·2H₂O</u>	<u>2.2g</u>
<u>KH₂PO₄</u>	<u>0.3g</u>
<u>MgCl₂·6H₂O</u>	<u>2.1g</u>
<u>Glucose</u>	<u>10 g</u>
<u>ddH₂O</u>	<u>1 l</u>

Preperfusion medium

<u>NaHCO₃</u>	<u>227 mg</u>
<u>10X GBSS</u>	<u>100 ml</u>
<u>ddH₂O</u>	<u>1l</u>

The solution was prepared directly prior to isolation; pH was adjusted to 7.4.

3.7 Isolation of rat liver Kupffer cells

Kupffer cells were also isolated and cultured according to previously described method (Tello et al., 2008). Liver macrophages were plated by using 200,000 cells/mL of culture medium (M-199) supplemented with 10% FCS. The medium was replaced 24 hours after isolation directly before irradiation. The cultured cells were maintained at 37°C in an atmosphere with 5 % CO₂ and 100 % humidity. Kupffer cells, on the first day after isolation were irradiated with 6 MV photons at a dose rate of 2.4 Gy /min using a Varian Clinac 600 C accelerator (Varian, Palo Alto, CA, USA). Single doses of 2 or 8 Gy were applied. For sham

irradiation, Kupffer cells were kept exactly the same time outside the incubator and in the same room as done for irradiation with 2 or 8 Gy.

3.8 Real-time polymerase chain reaction

3.8.1 RNA isolation for real-time-PCR analysis

3.8.1a RNA isolation procedure using silica columns

The isolation of total RNA from cultured rat liver hepatocytes, Kupffer cells and myofibroblasts was conducted using the NucleoSpin® RNAII kit (Macherey-Nagel) in accordance to the protocol for cultured animal cells.

3.8.1b Isolation of RNA by density-gradient ultracentrifugation

Total RNA was isolated from the liver by means of guanidine isothiocyanate extraction, cesium chloride density-gradient ultracentrifugation and ethanol precipitation according to method of Chirgwin (Chirgwin et al., 1979). This method is a versatile and efficient way to extract intact RNA from most tissues and cultured cells, even if the endogenous level of RNase is high.

Cell lysis: The cells were rapidly lysed in guanidine isothiocyanate-containing buffer, which ensures inactivation of RNases. The lysates were layered onto a CsCl gradient and spun in an ultracentrifuge. Proteins remain in the aqueous guanidine portion, DNA bands in the CsCl, and RNA settle down at the bottom of the tubes as a pellet. The RNA was recovered by dissolving the pellet. The recovery of RNA was usually excellent if the capacity of the gradient did not exceed.

Homogenization of the tissue sample: About 100 mg of frozen tissue was homogenized with Ultra-Turrax TP 18/10 homogenizer 3 times for 10 sec each

in 3 ml of ice-cold GITC buffer with freshly added Antifoam A (Sigma). The homogenates were centrifuged for 10 min at 3,500 rpm in a Rotixa /RP centrifuge (Hettich) at 4°C to pellet connective tissue and large cell debris.

CsCl gradient and ultra centrifugation: To prepare the gradient 2 ml of CsCl buffer was poured into 5-ml polyallomer ultracentrifuge tubes (6 per preparation). The cleared guanidine lysed samples were carefully layered on top of the CsCl buffer. The samples were centrifuged overnight (21 h) at 35,000 rpm in a Kontron TST55 rotor at 20°C. The supernatants were carefully removed by aspiration and the transparent gelatin-like RNA pellets were gently washed (preserving undisturbed) with 200 µl of 70% ethanol at room temperature. The pellets were reconstituted in 200 µl of RNase-free water by pipetting and transferred into sterile 1.5 ml eppendorf tubes and the procedure was immediately continued to RNA precipitation.

RNA precipitation: The RNA was precipitated with 450 µl of 100% ethanol in the presence of sodium acetate, pH 5.4 (20 µl of 2 M solution per pellet) overnight at -20°C. The RNA precipitates were centrifuged for 30 min at 12,000 rpm in an Eppendorf bench-top centrifuge at 4°C to get RNA pellet. Washing of the RNA pellet: Supernatants were discarded and pellet was washed with 200 µl of ice-cold 70% ethanol to remove all traces of sodium acetate. The RNA precipitates were centrifuged as described above, the supernatants were discarded and the pellet was dried for 30 min. at room temperature.

Reconstitution of RNA: The pellets were reconstituted in 100 µl of RNase-free water. To determine the concentration and purity of the RNA obtained, the aliquot of RNA sample was diluted 1:100 in RNase-free H₂O and the

concentration was measured at 260 nm and 280 nm by spectrophotometer (GeneQuant II, Pharmacia Biotech).

Solutions used for Ultracentrifugation

Guanidine isothiocyanate (GITC) buffer

<u>Guanidine isothiocyanate</u>	<u>4 M</u>
<u>0.25 M sodium citrate</u>	<u>25 mM</u>
<u>N-lauroylsarcosyl</u>	<u>0.5%</u>

The solution was sterile filtered and stored in the dark at 4°C. β -Mercaptoethanol was added just prior to use at a ratio of 1 to 100 μ l of GITC buffer.

Cesium chloride (CsCl) buffer

<u>Cesium chloride</u>	<u>5.7 M</u>
<u>0.25 M sodium citrate</u>	<u>25 mM</u>
<u>0.5 M EDTA</u>	<u>100 mM</u>

pH was adjusted with 0.25 M citric acid to 7.5; the solution was dissolved in RNase free H₂O, sterile filtered and stored at room temperature.

3.8.2 cDNA preparation by reverse transcription

The cDNA was generated by reverse transcription of 1 μ g of total RNA with 100 nM of dNTPs, 50 pM of primer oligo (dT)15, 200 U of moloney-murineleukemia virus reverse transcriptase (M-MLV RT), 16 U of protector RNase inhibitor, 1 \times RT buffer and 2.5 μ l of 0.1 M DTT for 1 hr at 40°C. Expression of LCN-2, α 2M, HO-1, SAA, IL-6, IL-1 β and TNF- α genes were analyzed using Platinum sybr Green qPCR mix UDG (Invitrogen). GAPDH, UBC and β -actin were used as housekeeping genes. Primer sequences used are given in Table 1.

Table 1: Primer sequences used for real-time PCR analysis

Gene	Forward 5' - 3'	Reverse 5' - 3'
Rat LCN – 2	GGA ATA TTC ACA GCT ACC CTC	TTG TTA TCC TTG AGG CCC AG
Rat α 2M	CTG TCA CTC ATC CTG TTG TC	ATC TCC TTC TTC GTG TCC TG
Mouse LCN – 2	AAA TT GCA CAG GTA TCC TCA G	CAG AGA AGA TGA TGT TGT CGT
Rat β actin	TGT CAC CAA CTG GGA CGA TA	AAC ACA GCC TGG ATG GCT AC
Rat Ubiquitin C	CAC CAA GAA CGT CAA ACA GGA A	AAG ACA CCT CCC CAT CAA ACC
Mouse GAPDH	AGA ACA TCA TCC CTG CAT CC	CAC ATT GGG GGT AGG AAC AC
Rat HO-1	CAA CCC CAC CAA GTT CAA ACA G	AAG GCG GTC TTA GCC TCT TCTG
Rat IL-6	GTC AAC TCC ATC TGC CCT TCA G	GGC AGT GGC TGT CAA CAA CAT
Rat TNF- α	ACA AGG CTG CCC CGA CTA T	CTC CTG GTA TGA AGT GGC AAA TC
Rat IL-1 β	TAC CTA TGT CTT GCC CGT GGA G	ATC ATC CCA CGA GTC ACA GAG G
Mouse SAA	TCATTTGTTCACGAGGCTTC	ATGGTGTCCCTCATGTCCCTTG

The cDNA samples are analyzed by Real Time PCR using the following ingredients for each PCR reaction:

Volume per reaction

"X" primer-forward (5mM) 0.5 μ l

"X" primer-reverse (5mM) 0.5 μ l

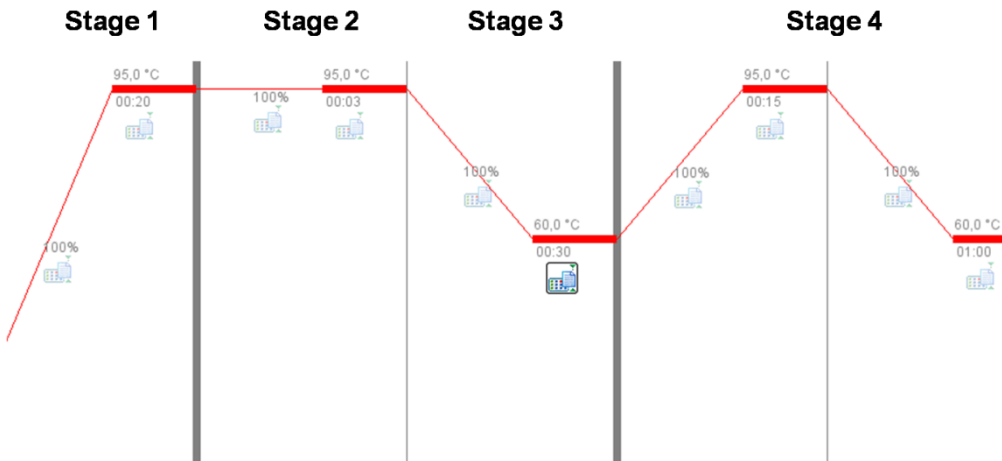
H₂O (Ampuwa®) 6.5 μ l

SYBR Green Master Mix Taq Polymerase 13.0 μ l

2.5 μ l of the cDNA sample or 2.5 μ l of H₂O for the negative control was added to each PCR reaction.

3.8.3 Thermal cycler amplification program

The amplification was performed at 95°C for 20 seconds, 95°C for 3 seconds to 60°C for 30 seconds for 40 thermal cycles in a Step one plus sequence detection system.



All samples were assayed in duplicate. Expression of different genes was analyzed using Platinum SYBR Green qPCR mix UDG. The PCR amplification program was followed by dissociation curve protocol for controlling the specificity of the PCR products. Specific temperature of dissociation of the PCR product was calculated by the Primer Express software. Curves of amplification were analyzed to measure the Ct value in the linear range of the amplification. The results were normalized to the house keeping gene and fold change expression was calculated using Ct values by Prism Graph Pad 5 software and Microsoft excel 2007.

3.8.4 Primer designing

Primers for different genes were designed using the program “Primer Express” (ABI System) and the gene bank data (<http://www.ncbi.nlm.nih.gov>). All the primer sets used for real-time PCR are listed in the Table 1.

3.8.5 Statistical analysis

The data were analyzed using Microsoft Excel 2007 and Graph pad Prism 5. Densitometric analysis was done by using Image-J. The results were normalized to the housekeeping gene and fold expression was calculated using threshold cycle (Ct) values. Experimental errors are shown as standard error of mean (SEM). Statistical significance was calculated by Student's t-test. Significance was accepted at $p \leq 0.05$.

3.9 Biochemical methods

3.9.1 Protein extraction from liver tissue and cultured hepatocytes

Preparation of tissue and cell lysates

All steps were performed at 4°C to prevent proteolytic degradation of the proteins. About 100 mg of frozen tissue and frozen cells were homogenized with Ultra-Turrax TP 18/10 model homogenizer 3 times for 10 sec each in 10 volumes of 50 mM Tris-HCl buffer, pH 7.4, containing 150 mM NaCl, 1 mM EDTA, 1% Triton X-100, 1mM PMSF, 1mM benzamidine, 1 μ g/ml leupeptin, 10 μ M chymostatin, 1 μ g/ml antipain, 1 μ g/ml pepstatin A. Crude homogenates were passed 5 times through a 22 G injection canula connected to a syringe. To pellet the nuclei and particular matter, crude homogenates were centrifuged for 5 min at 10,000 g (4°C) and the protein concentration of supernatants was determined by the bicinchoninic acid (BCA) method (Smith et al. 1985) using the BCA protein assay reagent kit (Pierce, Bonn, Germany). Prepared homogenates were dispensed in aliquots and stored at -20°C until use.

10X homogenization buffer (for tissue and cell processing)

<u>2 M Tris-HCl, pH 7.4</u>	<u>50 mM</u>
<u>0.5M EDTA</u>	<u>1mM</u>
<u>NaCl</u>	<u>150 mM</u>

1X homogenization buffer with additives

<u>10X homogenization buffer</u>	<u>1X</u>
<u>Triton X-100</u>	<u>1%</u>

Prior to use the following protease inhibitors were added:

<u>500 mM PMSF</u>	<u>1 mM</u>
<u>10 mg/ml leupeptin</u>	<u>1 µg/ml</u>
<u>1 M benzamidine</u>	<u>1 mM</u>
<u>8.25 mM chymostatin</u>	<u>8.25 µM</u>
<u>1 mg/ml pepstatin</u>	<u>1µg/ml</u>
<u>10 mg/ml antipain</u>	<u>1µg/ml</u>

3.9.2 Western blot analysis

Sample preparation

Aliquots of prepared tissue homogenates and cell lysates were denatured in sample buffer containing 2% SDS, 10% glycerol, 50 µg/ml bromphenol blue, 2% β-mercaptoethanol and 50 mM Tris-HCl, pH 6.8 by boiling at 95°C for 10 min and 15 µg of total protein was subjected to SDS-polyacrylamide gel electrophoresis (SDS-PAGE).

SDS-polyacrylamide gel

For all applications described, a 12.5% separating Tris/glycine SDS polyacrylamide ready made gel (SDS-PAGE) was used from invitrogen as instructed. The western blot was performed according to the method of Laemmli (Laemmli, 1970).

SDS-polyacrylamide gel electrophoresis (SDS-PAGE) and electrophoretic transfer

The samples were loaded onto the bottom of the wells. Electrophoresis was run at constant 20 mA per gel. The Rainbow™ colored protein markers (Amersham Pharmacia Biotech) were used as molecular weight standards. Electrophoretic transfer was carried out essentially as described by Towbin (Towbin et al. 1979). Prior to stopping the gel running, fiber pads, filter paper and nitrocellulose transfer membrane (0.45 µM pore size) were soaked in transfer buffer. After electrophoresis, the gel was removed out of the plates and immersed in transfer buffer. For electrophoretic transfer of proteins from the gel to a membrane, a Mini-Trans-Blot® Cell (Bio-Rad), compatible with described system for electrophoresis, was utilized. The transblot sandwich was assembled according to the manufacturer's instructions from Bio-Rad in the following order starting from the anode side: sponge, 2 sheets of filter paper, nitrocellulose membrane, gel, 2 sheets of filter paper, sponge. The assembled transblot sandwich was inserted into the transblot cell filled with transfer buffer. Ice-cooling unit was set behind the cathode side of transblot cell. The transfer ran for 2 h at 350 mA with one change of the ice-cooling unit after the first hour.

Immunovisualization

After transfer, the membrane was incubated on the rocking platform with blocking solution overnight at 4°C. Next, the membrane was incubated with primary antibody diluted in antibody dilution buffer for 2 h at room temperature. After washing (six times, five min on each occasion), the membrane was incubated with HRP-conjugated secondary antibody diluted in antibody dilution buffer for 1 h at room temperature. Afterwards, the membrane was washed as before. For the chemiluminescent detection SuperSignal® West Pico Chemiluminescent Substrate (Pierce) was used. Substrate working solution was prepared by mixing of equal volumes of two substrate components. The membrane was incubated with substrate working solution for 5 min at room temperature, laid between two sheets of transparent plastic protector and exposed to X-ray film, which was developed afterward according to the manufacturer's instructions.

Samples and loading buffer was used as instructed by invitrogen.

Blocking reagent

For 50 ml

Nonfat dry milk	2.5 g 5%
-----------------	----------

The solution should be prepared freshly and stored at 4°C.

Antibody incubation buffer

For 50 ml

5% nonfat milk	5 ml 0.5%
----------------	-----------

Primary antibodies were used in the following dilutions:

anti-LCN-2 mouse monoclonal antibody 1:300

anti-β-actin mouse monoclonal antibody 1:5000

Secondary antibodies were used in the following dilution:

Rabbit anti mouse HRP-conjugated 1:2000

3.10 Immunofluorescence staining

Cryostat sectioning (4 μ m) of frozen tissues was performed with liver or lung tissues, air dried and then fixed with cold acetone (-20°C). Immunofluorescence staining was performed as previously described (Malik et al., 2010). The tissues were incubated in a humidified chamber with fetal calf serum (FCS) for 1hour to avoid nonspecific staining. After 5 times washing with phosphate buffered saline (PBS) the liver or lung sections were incubated over night with mouse monoclonal anti-Lipocalin-2 antibody (Novus biological, NBPI-05182) and rabbit polyclonal myeloperoxidase (MPO) (Dako, A0398). On the next day after 5 times washing with PBS, the secondary antibody (Alexa flour 555 goat α mouse A21424, Invitrogen). Diamidino-2-phenylindole (DAPI) was used to counter stain the nuclei. Slides were covered with Fluoromount-G (0100-01, Southern Biotech).

Antibodies and chemicals were used in the following dilutions:

anti-LCN-2 mouse monoclonal primary antibody	1:100
anti-MPO rabbit polyclonal primary antibody	1:50
Goat anti mouse secondary antibody alexaflour 555	1:500
Goat anti rabbit secondary antibody alexaflour 488	1:1000
Diamidino-2-phenylindole (DAPI)	4 μ l in 100ml of PBS

3.11 Enzyme-Linked Immunosorbent Assay (ELISA)

To measure LCN-2 concentration in rat serum, Rat NGAL ELISA immunoassay kit 046 (Bioporto® Diagnostics, Gentofte, Denmark), based on solid phase ELISA, was used.

3.11.1 Reagent preparation

Since all samples should be pipette within 15 min, reagents needed for the assay were prepared prior to assay procedure. All reagents were provided with Bioporto® immunoassay kit.

Wash Solution: Dilute the 25x Wash Solution Conc. by pouring the total contents of the bottle (40 mL) into a 1-L graduated cylinder and add distilled or deionized water to a final volume of 1 L. Mix thoroughly and store at 2-8°C after use.

Sample Diluent: Dilute the 5x Sample Diluent Conc. by pouring the total contents of the bottle (50 mL) into a 250-mL graduated cylinder and add distilled or deionized water to a „final volume of 250 mL. Mix thoroughly and store at 2-8°C after use.

Rat NGAL Calibrators, Biotinylated Rat NGAL Antibody, HRP-Streptavidin, TMB Substrate, Stop Solution were ready to use.

3.11.2 Assay Procedure

100 µL volumes of each calibrator, diluted samples and any internal laboratory controls were pipette into their corresponding positions in the microwells. To synchronize the reaction in each well, all reagents were pipette using a multi-channel pipette. Wells were covered and incubated for 60 minutes at room

temperature on a shaking platform set at 200/minute. The contents of the microwells were aspirated and washed three times with 300 µL diluted Wash Solution. 100 µL of Biotinylated Rat NGAL Antibody was dispensed into each microwell. The wells were again covered and incubated for 60 minutes at room temperature on a shaking platform set at 200/minute. After washing 100 µL of HRP-Streptavidin was dispensed into each microwell and incubated for 60 minutes at room temperature on a shaking platform set at 200/minute. After washing step 100 µL of TMB Substrate was pipetted into each microwell. The wells were covered and incubated for exactly 10 minutes at room temperature in the dark. To stop the enzymatic reaction, 100 µL Stop Solution was added to each well, maintaining the same pipetting sequence as above and was mixed by gentle shaking for 20 seconds. Optical density of each well was determined within 30minutes by using a microplate reader (Dynatech Laboratories) at 450nm (reference wavelength 650 or 620 nm). The calculation of results was performed with a program (Dynatech MRX software, version 1.33) created in accordance to the manual instructions (Bioporto® immunoassay kit).

3.12 Safety Measures

All operations with genetically modified organisms and plasmid DNA were performed in accordance to the “Gentechnikgesetz” of 1990 and to the rules prescribed by the “Gentechnik-Sicherheitsverordnung” of 1990. Ethidium bromide, formaldehyde, DEPC and other chemicals deleterious for the environment, when used in the course of the work, were carefully managed and disposed properly in accordance with institutional guidelines. All the operations with radioactive chemicals were performed in a radioactivity class II laboratory

and the radioactive waste was disposed off according to the institutional instructions.

All chemicals used were of analytical grade and were purchased from commercial sources: Trizol reagent for isolation of RNA from the cells; real-time polymerase chain reaction (PCR) primers, M-MLV reverse transcriptase, reverse transcription buffer and 0.1 M DTT, platinum Sybr green Qpcr-UDG mix from Invitrogen, dNTPs, protector RNase inhibitor, bovine insulin, Klenow enzyme, primer oligo (DT)15 for cDNAsynthesis and alfa-32-p-labelled deoxycytidine triphosphate (specific activity 3000 Ci/mmol), NICK TM columns and Hybond N nylon membranes form Amersham Pharmacia Biotech (Freiburg, Germany). All other reagents and chemicals were from Sigma-Aldrich (Munich, Germany) or Merck (Darmstadt, Germany).

RESULTS

4.1 TO-induced Acute-phase-response

4.1.1 Serum LCN-2 concentration after TO injection in rat

Sera from control and TO-injected rats were analyzed to detect LCN-2 levels by ELISA (Figure 6). Serum LCN-2 concentration was not detectable in the control animals, and its levels remained nearly undetectable up to 6h in TO injected animals. Starting from the 12h experimental group, we found a significant increase in LCN-2 serum concentration ($7.25 \pm 2.94 \mu\text{g/ml}$) in TO-treated animals. We detected a further, progressive rise of serum LCN-2 levels at both 24h and 36h ($12.08 \pm 2.12 \mu\text{g/ml}$ and $18.7 \pm 3.13 \mu\text{g/ml}$ respectively). The highest value was detected 48h ($20.45 \pm 6.54 \mu\text{g/ml}$). This pattern of progressive elevation in LCN-2 serum concentration matches our findings in gene and protein expression, especially in liver tissue.

4.1.2 Changes in LCN-2 mRNA in liver from rats treated with turpentine oil:

Real-time PCR analysis of total RNA indicated relatively low levels of LCN-2 transcripts in normal control livers as compared to livers of treated animals (Figure 7). The difference in LCN-2 expression in control and treated animals remained insignificant until 4h after TO injection, when values started to increase significantly (7.8 ± 2.9 -fold), with further progressive, important increases at 6h (149.4 ± 9.4 -fold), 12h (4059.6 ± 420.8 -fold) and 24h (6960.3 ± 1091.4 -fold). After 36 h, gene expression reached a peak (8738.2 ± 2103.7 -

fold), followed by a slight decrease, but remained significantly elevated up to 48h. This dramatic increase was seen in all series of TO-treated animals with highly significant results.

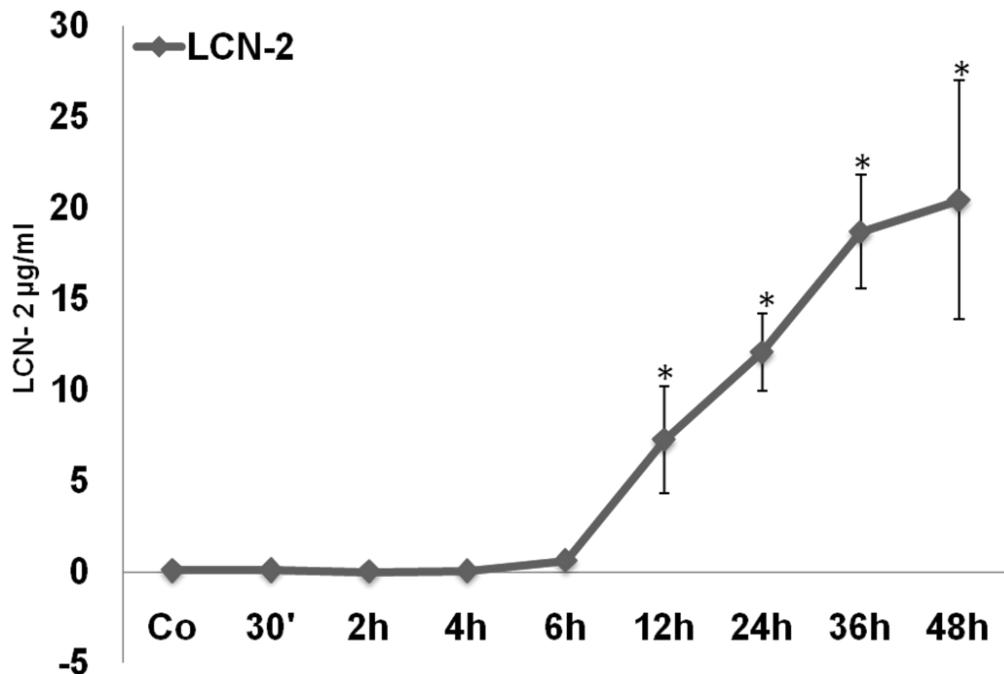


Figure 6: Changes in LCN-2 serum level during APR determined by ELISA. Results are shown in fold \pm standard error of mean (SEM) (* $P \leq 0.05$ analyzed by Student's t-test, $n=3$).

4.1.3 Changes in α 2M and HO-1 mRNA in liver from TO-treated rats

In order to better define LCN-2 gene expression behaviour and compare it with other, classical acute phase proteins, we also investigated the kinetics of α 2M (known major secretory protein) and HO-1 (intracellular protein) which are the main positive acute phase proteins in the rat (Figure 7). The purpose to use major acute phase proteins was to compare the LCN-2 expression under acute

phase conditions due to its strong induction on serum levels. Like LCN-2, the α 2M and HO-1 level of transcripts was relatively low in the control animals and did not show any significant increase until 4h after injection (59.9 ± 23.9 and 17.3 ± 1.28 -fold). A peak in α 2M gene expression was reached at 12h (1024.7 ± 264.1 -fold), followed by a slow decrease that did not yet bring transcript products to basal levels by 48h (565.3 ± 120.9 -fold). The behaviour of LCN-2 and α 2M gene expression was similar but with a different fold increase of LCN-2 which was expressed approximately 7000-fold more than α 2M. HO-1 gene expression showed a maximum increase at 6h (48 ± 6.09 -fold), followed by down-regulation, and after 12h the decrease brought transcript products to basal levels. The gene expression of α 2M, HO-1 and LCN-2 showed a significant difference where the LCN-2 expression is very strong as compared to these known acute phase proteins.

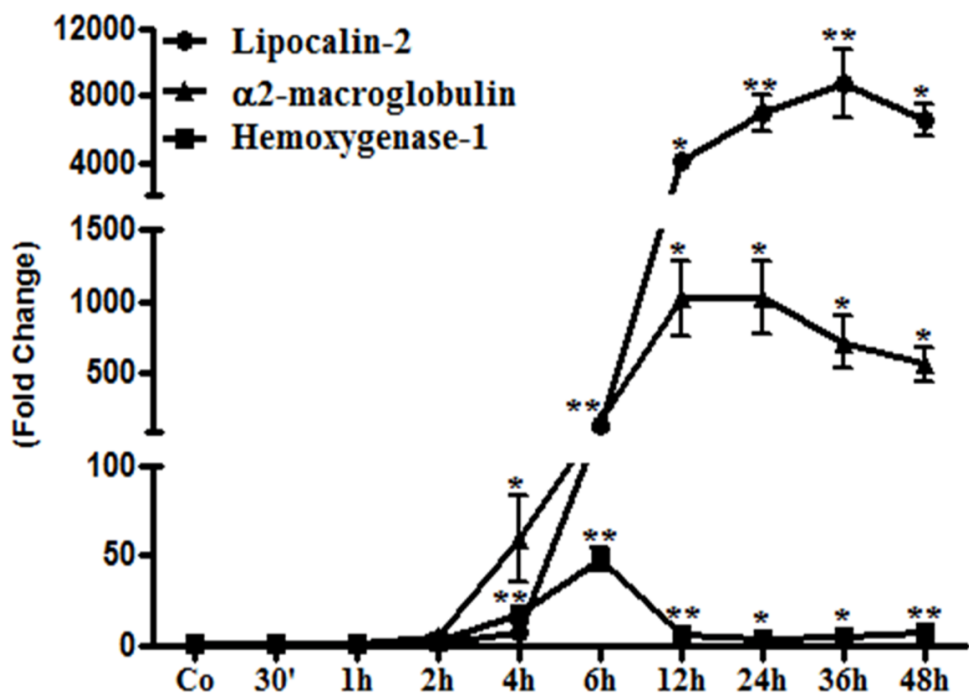


Figure 7: Changes in gene expression of LCN-2, α 2M and HO-1 mRNA in liver tissue of TO-injected rats determined by Real Time Polymerase Chain Reaction

(PCR) analysis. The results were normalized to the housekeeping gene, i.e. beta actin, fold change expression was calculated using threshold cycle (Ct) values and experimental errors are shown as \pm SEM (* $p \leq 0.05$, ** $p \leq 0.005$, *** $p \leq 0.0005$ analyzed by Student's t-test, n = 4).

4.1.4 Changes in LCN-2 mRNA in kidney and other organs from TO-treated rats

LCN-2 is widely indicated as an acute and chronic kidney injury marker in various pathological conditions (Han and Bonventre, 2004; Viau et al., 2010). We therefore investigated LCN-2 gene expression in the kidney tissue of TO-treated animals (data did not show). Basal transcript levels in kidney were higher than in liver tissue (25.5 ± 1.4 PCR threshold values). The PCR threshold value came up to 22.2 ± 1.6 (5.12 ± 2.16 -fold) at 12h but this change was not significant in any of the series. Furthermore, with other organs heart, spleen, lung and brain also LCN-2 showed no considerable change if compared to the liver (Table 2). The expression of LCN-2 was maximal at 24h up to 2.45 ± 0.12 -fold in heart, at 12h in brain (35.59 ± 6.71 -fold), at 6h in spleen (8.63 ± 1.61 -fold) and at 12h in lung (21.63 ± 0.19 -fold). This comparison of LCN-2 expression in major organs showed a clear difference between the liver and other organs of TO-treated rats. These results confirm our hypothesis that liver is the major source of LCN-2 production.

Table 2: Changes in LCN2 gene expression in liver, kidney, heart, brain, spleen and lung. Results are shown in fold \pm SEM (n=3).

Time point	Liver	Kidney	Heart	Brain	Spleen	Lung
2h	1.19±0.24	1.36±0.09	0.17±0.10	2.27±0.29	0.1±0.005	3.68±0.54
4h	7.9±1.4	1.39±0.17	2.43±0.08	2.64±0.91	0.13±0.002	5.51±2.34
6h	149±9	1.35±0.28	2.18±0.05	3.66±0.77	8.63±1.61	4.43±0.17
12h	4059±421	5.12±2.16	11.1±0.58	35.59±6.71	5.44±0.29	21.63±0.19
24h	6960±1091	3.36±0.36	2.45±0.12	9.37±3.07	4.86±0.36	4.37±0.53
36h	8738±2104	2.53±0.55	1.61±0.09	6.38±2.28	1.09±0.002	2.69±0.13

4.1.5 Changes in LCN-2 tissue protein in liver from TO-treated rats

Western blot analysis of total liver homogenate showed a progressive increase of LCN-2 protein content in the liver, which became clearly evident 12h after the TO injection similar to the RNA data. LCN-2 protein expression then started to increased further and showed a very specific strong band of LCN-2 after 36h. α2M protein expression was very low as compared to LCN-2. Although α2M protein expression also increased after 12h and reached a maximum after 36h but the intensity of expression was lower but the pattern of increase was similar to LCN-2. HO-1, a positive acute phase protein, did not show a strong protein expression at any time point. Its weak expression can be seen to be induced after 12h as in α2M and LCN-2 but was not convincing compared with LCN-2 (Figure 10).

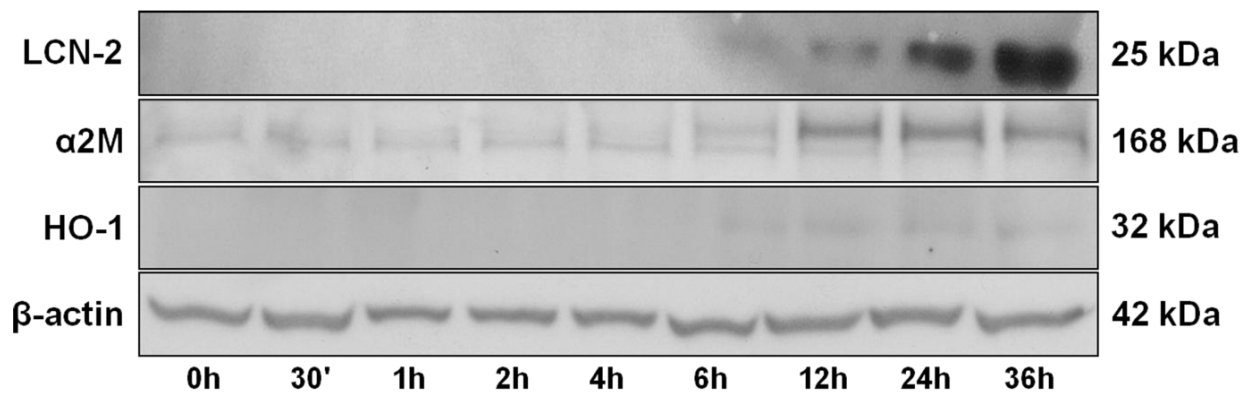


Figure 8: Western blot analysis of LCN-2 (25 kDa), α 2M (168 kDa) and HO-1 (32 kDa) from total protein of TO-treated rat liver. β -actin (42 kDa) was used as loading control.

4.1.6 Changes in LCN2 m-RNA in livers of TO-treated wild type and knock-out mice as compared to SAA

To further investigate the role of IL-6 in LCN-2 gene expression, TO-treated wild type and IL-6 knock-out mice were used. Total RNA from the livers of TO-treated wild type and IL-6 knock-out mice was analysed by RT-PCR (Figure 9). Furthermore, LCN-2 gene expression was compared to SAA, the major acute phase protein of mice. The purpose for comparison with SAA was to determine whether LCN-2 is also the major acute phase protein in mice, as we determined a strong expression in our rat model of tissue damage. LCN-2 expression in untreated control wild type and IL-6 knock-out mice was 24.11 ± 0.43 and 24.6 ± 0.13 PCR threshold cycle values, respectively. Starting 2h after TO injection, the wild type animals showed a significant and progressive up-regulation of LCN-2 gene expression which reached a peak at 12h and 24h (2274 ± 298 and 2498 ± 82 -fold respectively). The increased expression was highly significant. In IL-6 knock-out mice, LCN-2 transcript levels only increased

slightly to a maximum of 26.3 ± 12.4 -fold at 12h. After 12h, LCN-2 expression started to decrease until it reached the basal levels.

SAA behaved in a similar way to LCN-2 in wild type and IL-6 knock-out mice. In wild type mice SAA expression started to increase after 2h and its transcripts levels reached a maximum at 24h (2825 ± 135 -fold) which was a significant increase. In IL-6 knock-out mice SAA was expressed up to 30-fold after 6h and its expression did maximally increase at 12h up to 23.4 ± 6.07 -fold followed by a decrease.

4.1.7 Changes in IL-6, IL-1 β and TNF- α expression in injured TO-treated rat muscle

The location of the induced damage is very important to determine the effect and type of mediators (know as cytokines) for the induction of acute phase response, triggered at that site. To analyse the effect of cytokines on the place of damage, mRNA from injured rat muscles were used along with controls. We analysed the expression of three major acute phase cytokines IL-6, IL-1 β and TNF- α in TO-induced damaged muscle. In the injured muscle, IL-6 started to increase at 2h (147 ± 69 -fold) and its expression reached the highest level at 4h and 6h ,which was significant (1055 ± 173 and 1982 ± 289 -fold, respectively). After 12h IL-6 expression started to decrease but did not reached at basal levels. On the other hand, IL-1 β was significantly expressed maximally at 6h (425 ± 55 -fold) followed by a decrease in expression. TNF- α did not show any significant increase and it did only reached a maximum of up to 3.6 ± 0.9 -fold at 4h (Figure 10). The expression of IL-6 was major but we cannot exclude a role of IL-1 β . Although the expression of IL-1 β was much less than IL-6, the fold

increase was considerable. Here, we can exclude the role of TNF- α , as it did not show any significant results.

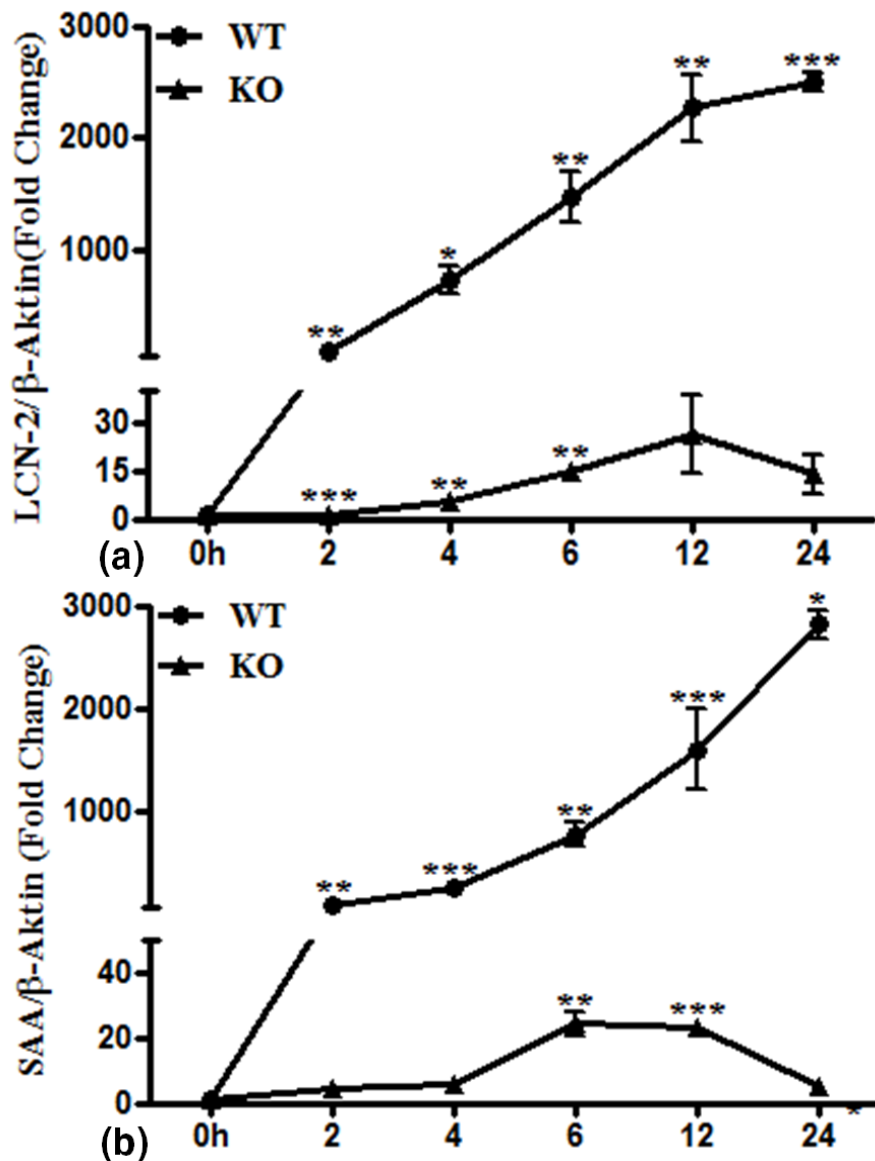


Figure 9: Changes in gene expression of (a) LCN-2 and (b) SAA in wild type and IL-6 knock-out mice. The results were normalized to the housekeeping gene, i.e. GAPDH, and shown in fold \pm SEM (* p \leq 0.05, ** p \leq 0.005, ***p \leq 0.0005 analyzed by Student's t-test, n=3.

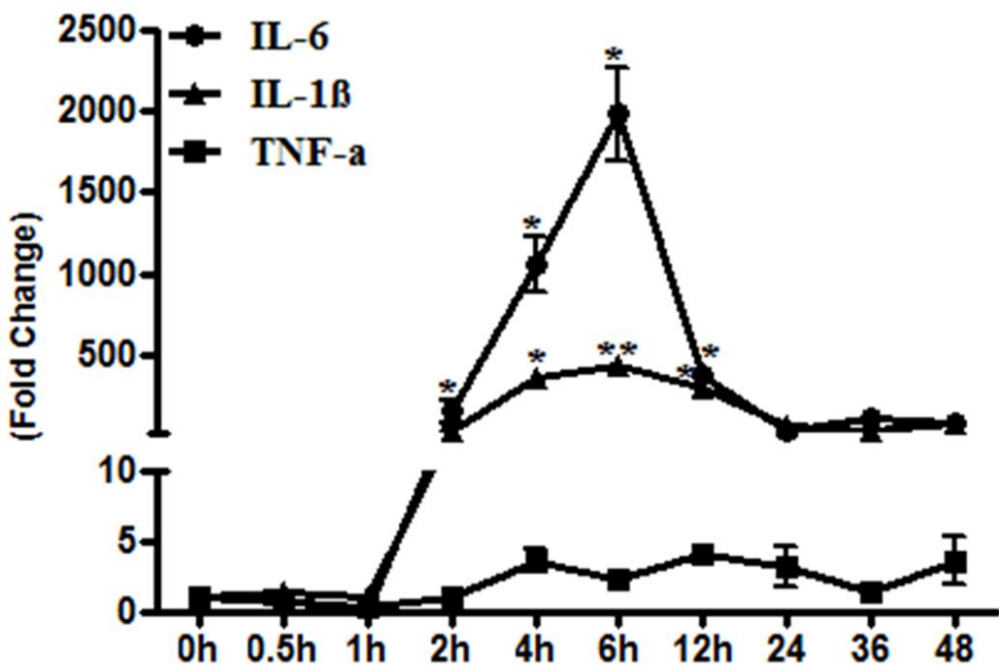


Figure 10: Changes in gene expression of IL-6, IL-1 β and TNF- α in injured TO-injected rat muscle. The results were normalized to the housekeeping gene, i.e. β -actin and shown in fold \pm SEM (* p \leq 0.05, ** p \leq 0.005, ***p \leq 0.0005 analyzed by Student's t-test, n=3).

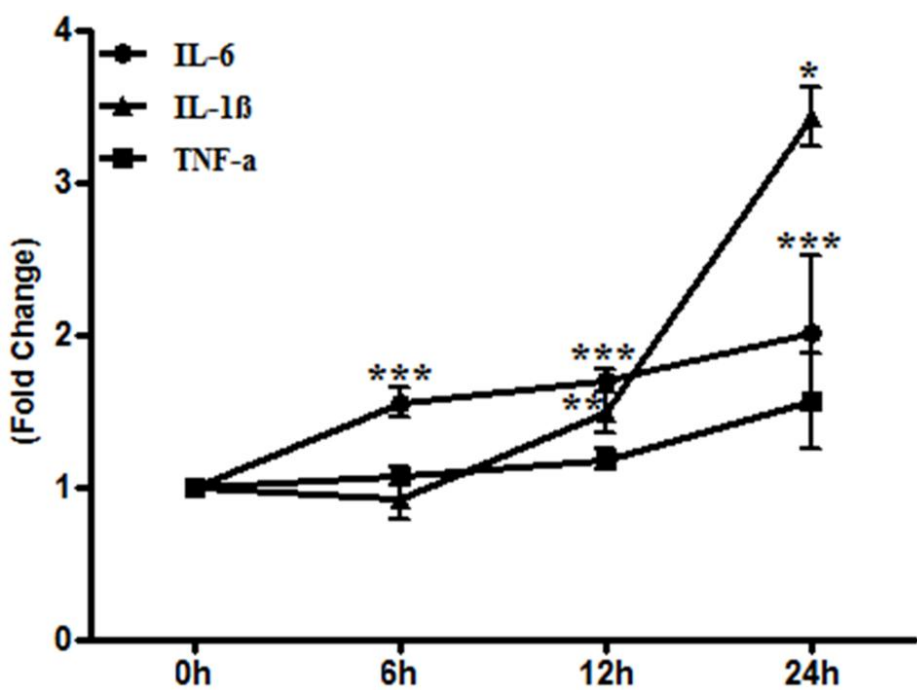


Figure 11: Changes in gene expression of IL-6, IL-1 β and TNF- α treated hepatocytes. The results were normalized to the housekeeping gene, i.e. β -actin

and shown in fold \pm SEM (* p \leq 0.05, ** p \leq 0.005, ***p \leq 0.0005 analyzed by Student's t-test, n=3).

4.1.8 Changes in LCN-2 m-RNA and protein in cytokine-treated rat hepatocytes

To confirm whether IL-6 is the main cytokine inducing LCN-2 and to find out which liver cells were responsible for its induction, we isolated hepatocytes, myofibroblasts and Kupffer cells and treated them with different cytokines (IL-6, IL-1 β and TNF- α). Real-time PCR analysis of total RNA from IL-6 treated cultured cells showed a significant up-regulation (1.55 \pm 0.18-fold) at an early time point i.e. 6h as compared to IL-1 β and TNF- α (0.92 \pm 0.24 and 1.07 \pm 0.16-fold respectively), which reached a maximum at 24h (2.02 \pm 0.14-fold; Figure 11). LCN-2 expression in IL-1 β treated hepatocytes reached a maximum after 24h but the results were not as significant as were in IL-6 treated rat hepatocytes.

Furthermore, total protein was extracted from cytokine-treated rat hepatocytes to determine the LCN-2 protein expression. Western blot analysis of untreated hepatocytes showed that LCN-2 expression was already present in the controls. After cytokine treatment with IL-6, IL-1 β and TNF- α , the LCN-2 expression increased significantly in the IL-6 treated hepatocytes after 6h and it reached a maximum after 24h. Densitometric analysis showed that the values were highly significant (Figure 12). IL-1 β and TNF- α also showed a significant up-regulation of LCN-2 protein expression which was more obvious in IL-1 β as compared to TNF- α . Overall IL-6 treated rat hepatocytes showed the highest LCN-2 expression.

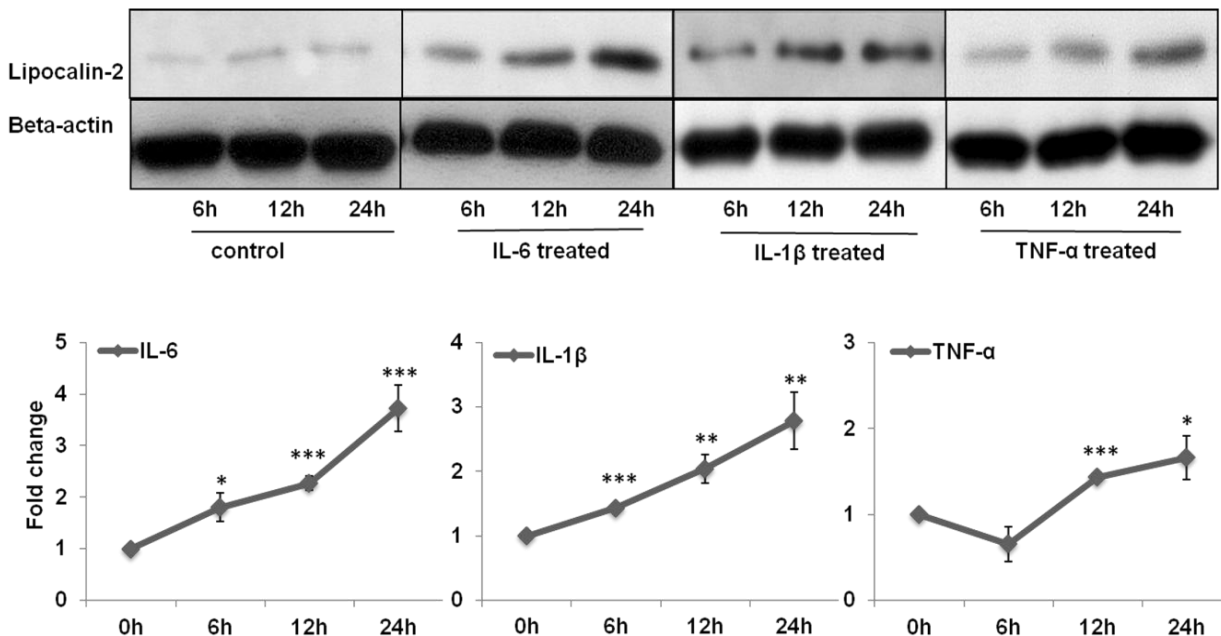


Figure 12: Western blot analysis of IL-6-, IL-1 β - and TNF- α -treated hepatocytes with LCN-2 at 6, 12 and 24h along with control. Densitometric analysis of Western blots was also performed to show the changes in protein expression of LCN-2. Results are shown in fold \pm SEM (* p \leq 0.05, ** p \leq 0.005, ***p \leq 0.0005 analyzed by Student's t-test, n=3).

The CT value (Threshold cycle) is defined as the fractional cycle number at which the fluorescence passes the fixed threshold. The higher the CT value is for the specific gene at a given time, the lower the abundance is for the specific mRNA (Malik et al., 2010). Although the fold increase in the amounts of specific mRNA gives an idea of the changes in expression of LCN-2 in hepatocytes induced by IL-6, comparison of the Ct values provides an indirect indication of relative LCN-2 gene expression in control liver tissue (27.65 ± 0.36) and untreated hepatocytes (13.40 ± 0.43), and may provide an additional insight with regard to why the magnitude of changes induced by IL-6 *invivo* cannot be achieved *in vitro*. One can appreciate the huge induction of LCN-2 during isolation and culturing of hepatocytes. That is why, only a small change can

further be induced by IL-6 treatment. This means that the fold change alone would underestimate/depreciate the real effect of IL-6 (Table 3) which was observed *in vivo* (Figure 10). The same effect can be seen in α2M and to some extent HO-1 (in comparison with LCN-2) but the total liver and IL-6 treated hepatocytes mRNA levels of LCN-2 have the lowest Ct, which further confirms our data.

Table 3: Threshold cycle (Ct) values of RT-PCR analysis of LCN-2, α2M and HO-1 in total liver tissue (upper part) and IL-6 treated hepatocytes (lower part) mRNA (Ctmean ±SEM) (n=3).

Total Liver mRNA (Ct)			
	LCN-2	α2M	HO-1
0h	27,65±0,36	28,13±0,50	28,76±0,96
30min	26,57±0,35	27,92±0,75	28,55±0,56
1h	27,62±0,42	26,82±1,19	27,98±1,01
2h	27,32±0,53	26,13±0,07	25,64±0,67
4h	23,95±0,69	23,74±2,18	24,87±0,89
6h	19,26±0,56	21,14±0,57	21,14±0,78
12h	15,70±0,23	17,71±0,74	22,98±0,99
24h	15,10±0,41	18,63±0,07	22,02±1,03
36h	14,01±0,71	19,23±1,17	25,43±1,15
48h	15,81±0,76	19,62±0,84	25,72±0,93

IL-6 treated Hepatocytes mRNA (Ct)			
	LCN-2	α2M	HO-1
0h	13,40±0,43	16,67±0,28	24,83±0,54
6h	12,77±0,09	14,70±0,63	23,32±0,20
12h	12,49±0,50	14,06±0,70	23,36±0,58
24h	11,94±0,47	15,06±1,89	22,86±0,69

4.2 Irradiation induced Liver damage

4.2.1 Serum Lipocalin-2 concentration after liver irradiation

LCN-2 serum levels were detected by ELISA in control and irradiated animals.

LCN-2 serum levels started to increase significantly within 1h after direct liver irradiation (Figure 13) and reached a significant maximum within 6h (2.5 µg/ml \pm 0.6-fold). After 6h, the Lipocalin-2 serum levels started to decrease. The overall results were significant and LCN-2 serum level were reproducible in every series.

Lipocalin-2 ELISA results were further confirmed by Western blot analysis of serum proteins (Figure 14). Sera collected from control and irradiated animals showed approximately the same results as were seen in ELISA. One can see the maximum expression of LCN-2 at 6h in ELISA and Western blot serum analysis followed by decrease in expression.

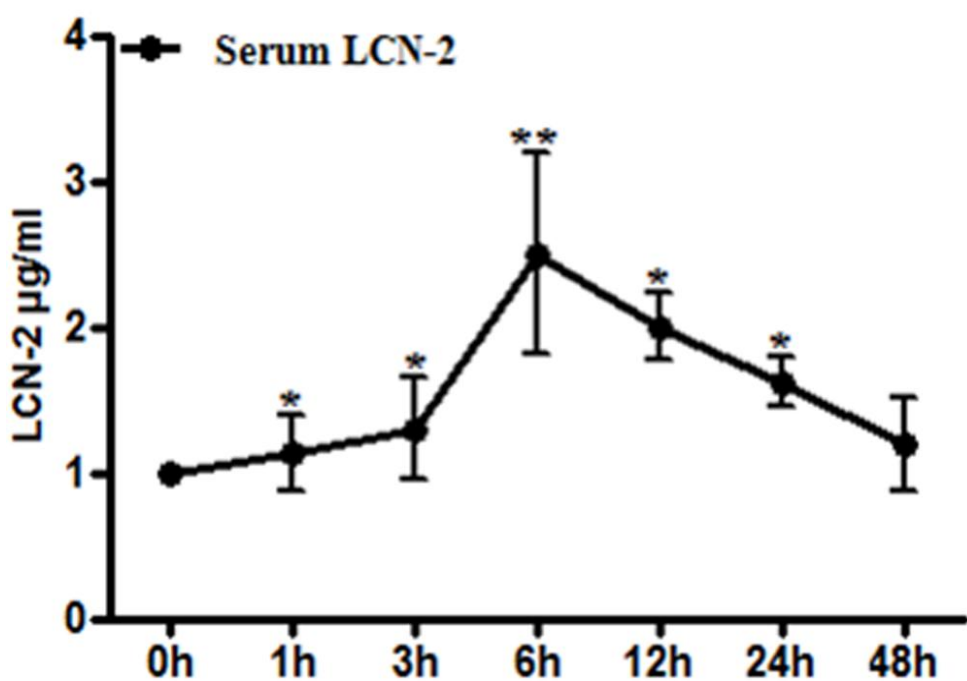


Figure 13: Changes in LCN-2 serum level during irradiation determined by ELISA. Results of ELISA are shown in $\mu\text{g/ml} \pm$ standard error of mean (SEM) (* $P \leq 0.05$, (** $P \leq 0.005$ analyzed by Student's t-test, n=3).

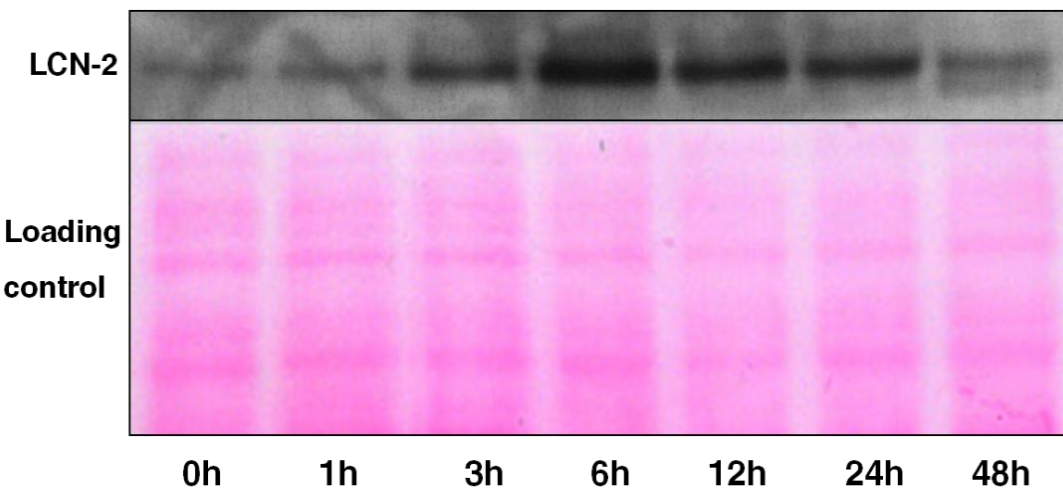


Figure 14: Changes in LCN-2 serum level during irradiation determined by ELISA Western blot analysis. (LCN-2 25kDa with loading control)

4.2.2 LCN-2 immunostaining in irradiated liver tissue

The immunofluorescence staining of cryostat sections of irradiated liver tissue (Figure 15) was performed to determine the LCN-2 localization during acute-phase-response. The liver sections were stained with LCN-2 primary antibody followed by a fluorescent secondary antibody. The results showed a recruitment of LCN-2+ cells within 1h followed by an increased accumulation of LCN-2+ cells around the portal and central areas within 1, 6, and 24h after irradiation as compared to normal sham-irradiated animals of every time point (only one control is shown here). One can see that the recruited LCN-2+ cells are moving within the given time-scale towards the central and portal fields to be secreted into the serum and trigger an acute-phase-response. Control liver tissue has some LCN-2+ cells which suggest that LCN-2 can be involved in normal tissue functions.

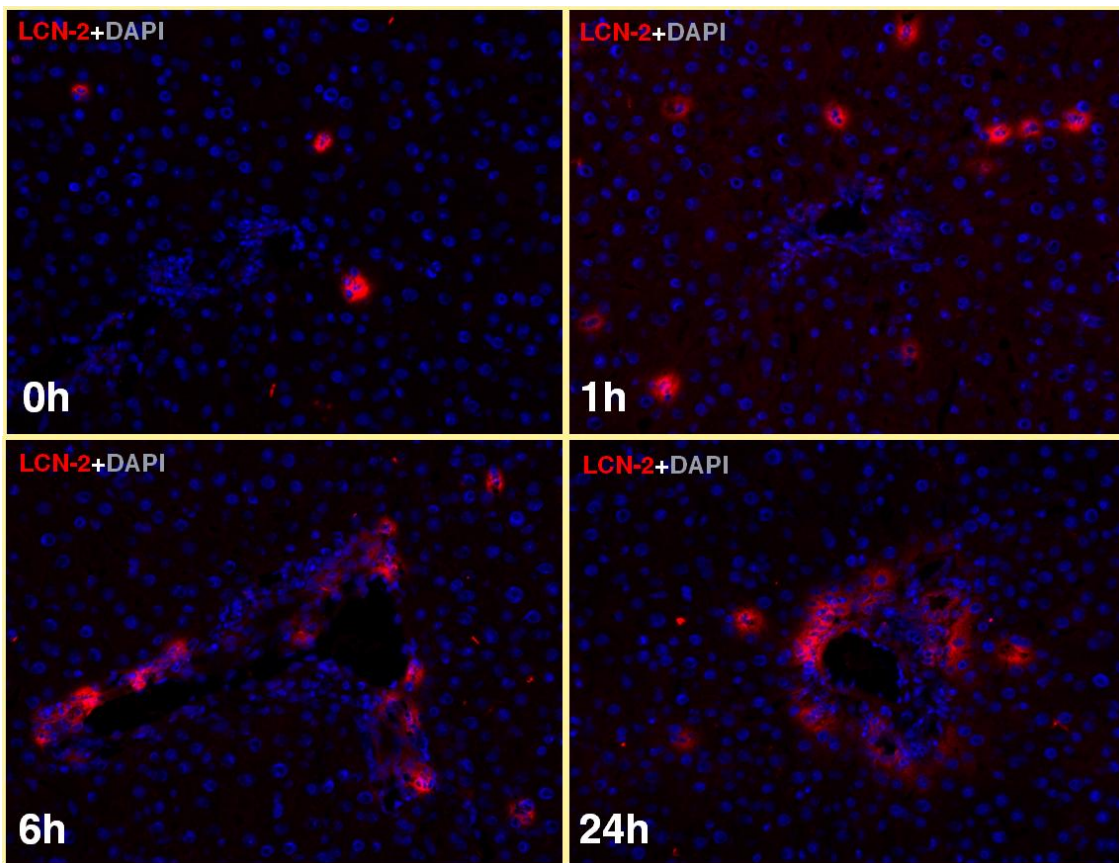


Figure 15: Immunofluorescence detection of Lipocalin-2 positivity in liver of normal sham irradiated control rats, 1, 6 and 24 hours after irradiation. Sections were stained with an antibody against neutrophil gelatinase associated Lipocalin-2 followed by fluorescence immunodetection (original magnification 200x).

4.2.3 Real-time PCR analysis of total RNA from rat liver

In order to determine LCN-2 gene expression in control and irradiated animal, RNA from total tissue was extracted and used to make cDNA for Real time PCR analysis. LCN-2 transcripts in normal control livers were very low as compared to livers of irradiated animals (Figure 16). LCN-2 expression started to increase significantly within 1h (4.31 ± 1.16 -fold), which increased further and reached its maximum level within 12h and 24h (536 ± 111 and 551 ± 108 -fold respectively)

followed by a decrease. The fold increase was high and highly significant. This confirmed our results of immunofluorescence staining in irradiated rat tissue section.

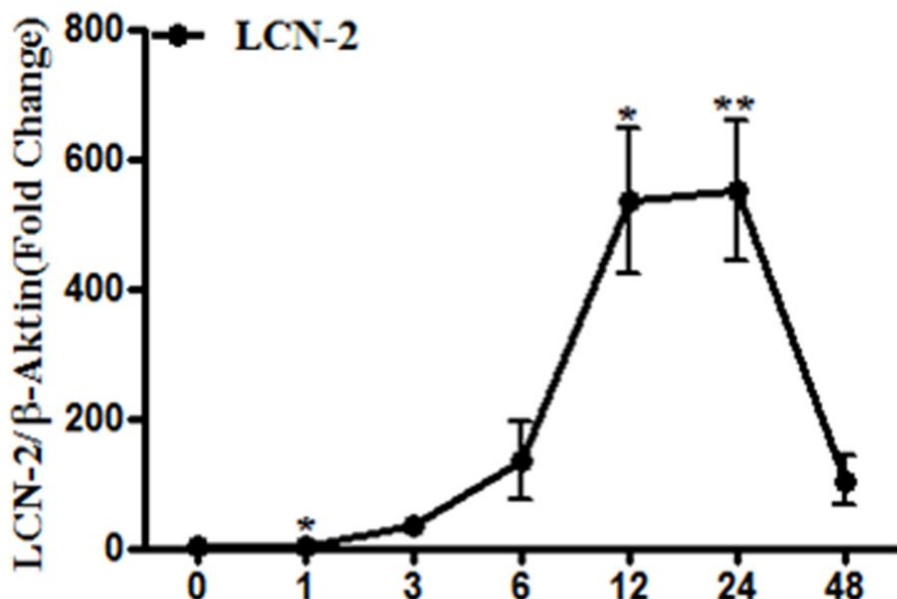


Figure 16: Fold changes of mRNA expression of Lipocalin-2 in irradiated liver tissue at time points from 1 hour to 48 hours related to normal sham irradiated control rats determined by Real Time Polymerase Chain Reaction (PCR). The results were normalized to the housekeeping gene, i.e. β -actin, fold change expression was calculated using threshold cycle (CT) values and experimental errors are shown as \pm SEM (* $p \leq 0.05$, ** $p \leq 0.005$, *** $p \leq 0.0005$ analyzed by Student's t-test, $n = 3$).

4.2.4 Western blot analysis of rat liver proteins

Western blot analysis of total liver homogenate showed a dramatic increase after 1h of irradiation (Figure 17). It stayed up-regulated up to 24h and then decreased after 48h. This increased expression of protein was comparable with serum levels and gene expression of LCN-2.

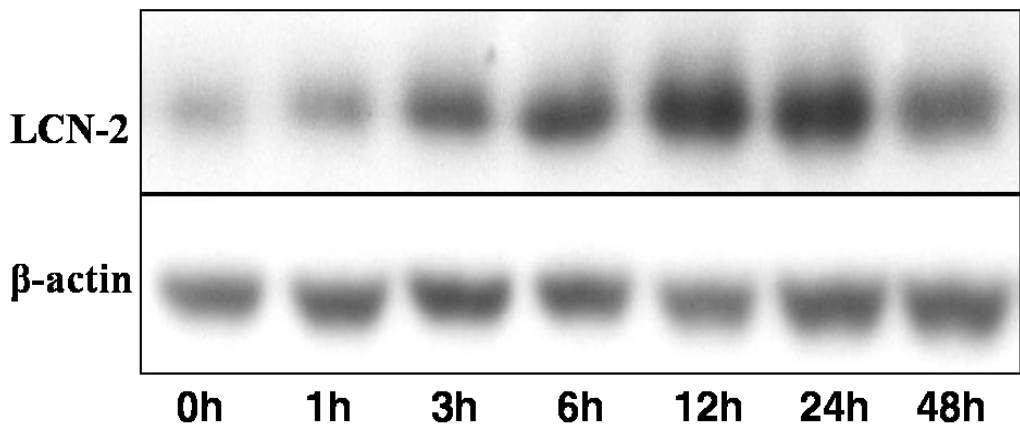


Figure 17: Western blot analysis of LCN-2 (25 kDa) from total protein of different timepoints from irradiated liver including normal sham irradiated animals. Beta actin (42 kDa) was used as loading control.

4.2.5 Real-time PCR analysis of rat irradiated hepatocytes, myofibroblasts and Kupffer cells

To determine the major liver cell type responsible to induce LCN-2 during irradiation we isolated hepatocytes, myofibroblasts and Kupffer cells and irradiated them with 8 Gray (Figure 18). Irradiated hepatocytes showed a slight increase in LCN-2 expression right after irradiation at 1 hour (1.08 ± 0.41 -fold) which became pronounced within 6 and 12 hours (2.01 ± 0.24 - and 2.19 ± 0.25 -fold respectively) followed by LCN-2 decrease. Kupffer cells showed a slight but significant increase of LCN-2 expression within 3 hours (1.53 ± 0.37 -fold) followed by decrease. Myofibroblasts exposed to radiation showed a significantly decreased LCN-2 expression which remained during the observation time. Among all the liver cell types, hepatocytes seemed to be more involved with LCN-2 expression and we showed above that hepatocytes are responsible for LCN-2 induction along with cytokines.

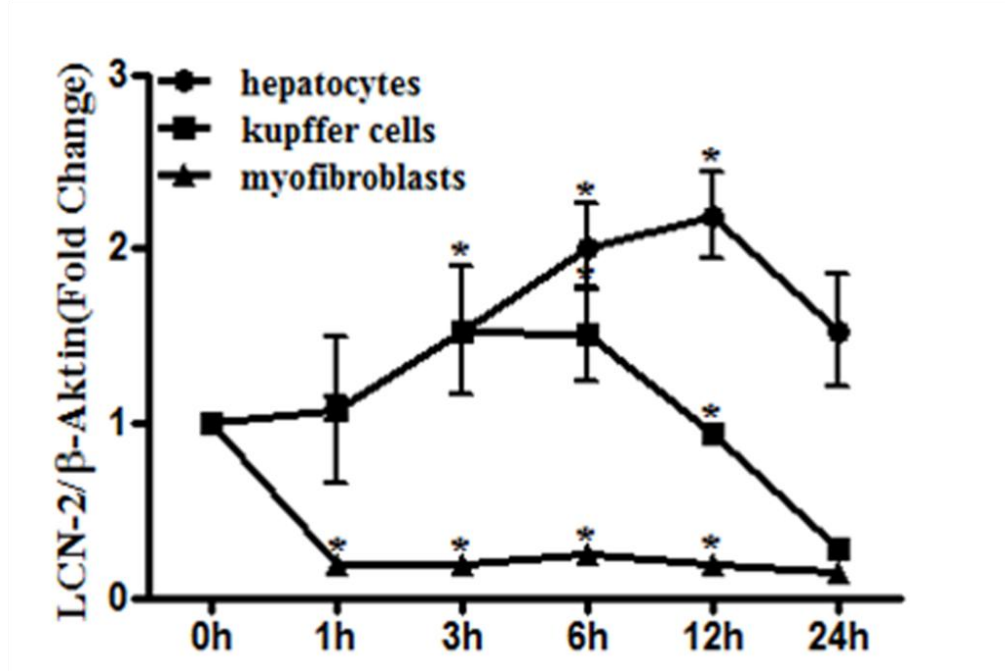


Figure 18: Fold changes of mRNA expression of LCN-2 in different irradiated liver cells (hepatocytes, myofibroblasts and Kupffer cells) at different time points related to normal sham irradiated control cells determined by real time polymerase chain reaction (PCR). The results were normalized to the housekeeping gene, i.e. beta actin, fold change expression was calculated using threshold cycle (C_t) values and experimental errors are shown as \pm SEM (* $p \leq 0.05$, ** $p \leq 0.005$, *** $p \leq 0.0005$ analyzed by Student's t-test, $n = 3$).

4.2.6 Real-time PCR analysis of rat irradiated hepatocytes treated with different cytokines

From our *in vitro* experiments which show that within the liver cells hepatocytes are the major source of more LCN-2 expression, we tried to find out the major acute phase cytokine responsible for this significant expression. For this purpose we treated our hepatocytes with different acute phase cytokines (IL-6, IL-1 β , TNF α and IL-6+TNF- α) along with irradiation (8Gy).

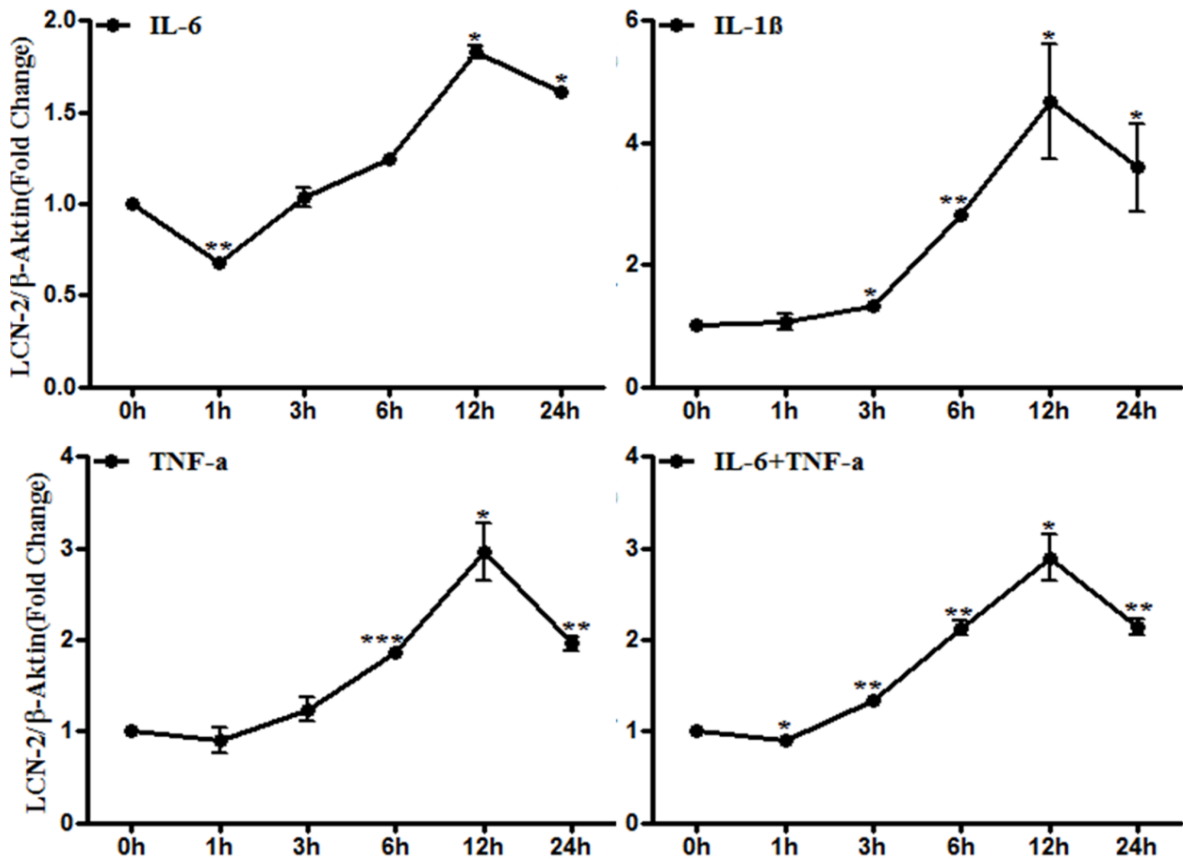


Figure 19: Fold changes of mRNA expression of LCN-2 in IL-6-, IL-1 β -, TNF- α - and IL-6+TNF- α -treated hepatocytes. The results were normalized to the housekeeping gene, i.e. β -actin, and are shown as \pm SEM (* p \leq 0.05, ** p \leq 0.005, ***p \leq 0.0005 analyzed by Student's t-test, n = 3).

PCR analysis from these hepatocytes showed that irradiated hepatocytes treated with IL-1 β showed a higher LCN-2 expression among all other cytokines though the difference was not much. IL-1 β treated irradiated hepatocytes showed a significantly elevated LCN-2 expression directly after irradiation, reaching its maximum within 12 hours (4.67 ± 0.94 -fold) followed by a drop in LCN-2 expression. IL-6, TNF- α and IL-6+TNF- α treated irradiated hepatocytes also showed an increase in LCN-2 expression with a maximum at 12 hours (1.82 ± 0.04 -, 2.96 ± 0.31 - and 2.89 ± 0.25 -fold respectively) and a decrease at

24 hours (Figure 19). In comparison with all cytokines, IL-1 β induced LCN-2 expression most and even IL-6 and TNF- α together could not enhance the LCN-2 expression induced by IL-1 β .

4.3 Irradiation induced Lung damage

4.3.1 Serum Lipocalin-2 concentration after lung irradiation

Sera from control and irradiated animals were collected and analyzed for LCN-2 serum levels. We could not find any serum level of LCN-2 in lung even after irradiation by ELISA in any series. Furthermore, we tried to determine LCN-2 serum levels by Western blot analysis but the results remained the same.

4.3.2 LCN-2 Immunostaining in irradiated lung tissue

The immunofluorescence staining of cryostat sections of irradiated lung tissue was performed to determine the LCN-2 localization after lung irradiation. Immunofluorescence staining of the lung tissue sections (Figure 20) showed a strong constitutive LCN-2 expression. The control and each time point after irradiation showed a considerable expression of the LCN-2 + cells. The LCN-2 localization seemed to be more around the alveolar areas. To be sure that LCN-2 positivity is true and not an artifact, we took another known marker of granulocytes i.e. myeloperoxidase (Amanzada et al., 2011; Le, V et al., 1997). and stained it along with the LCN-2 primary antibody in a double immunofluorescence staining. The double positivity and overlapped expression of both markers confirmed the true positivity of LCN-2 (Figure 20) and proved the fact that LCN-2 is a marker of granulocytes. The strong LCN-2 expression in

control lung tissue sections showed that the lung has already protection against external pathogens prior to any stress.

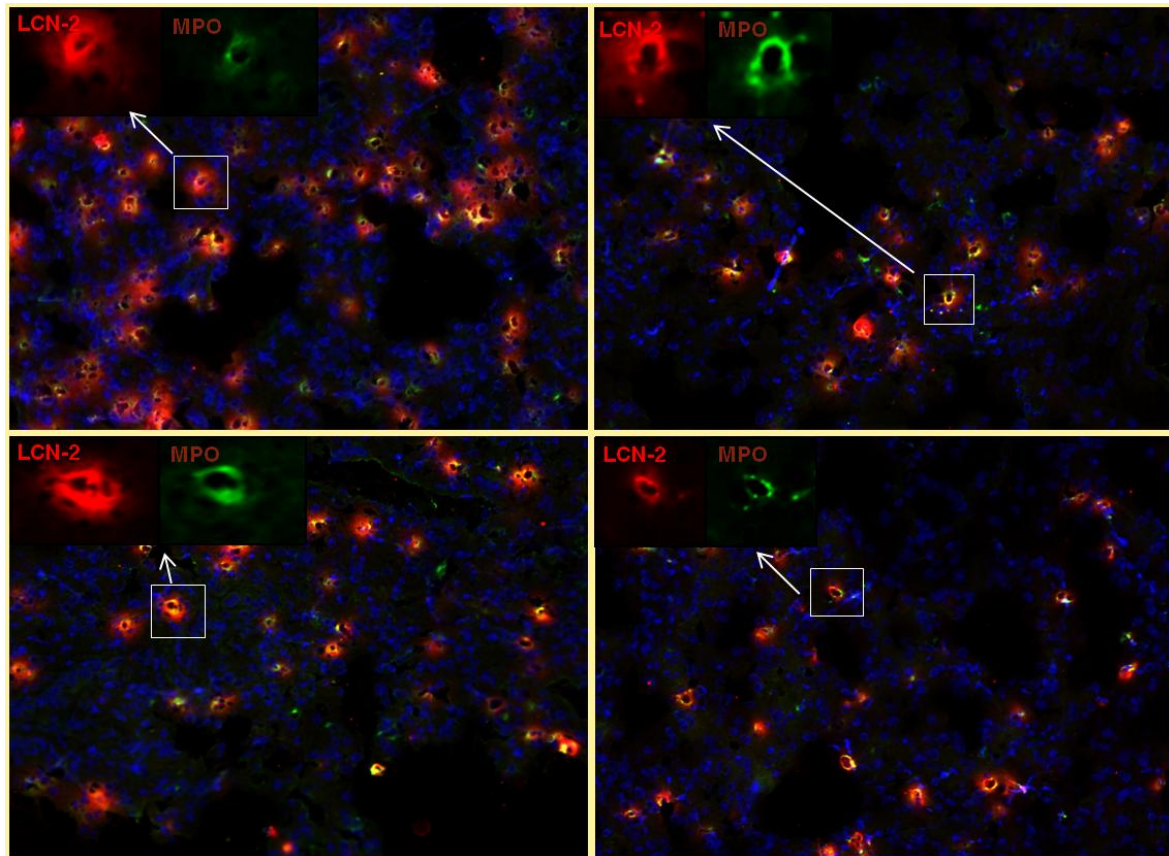


Figure 20: Double Immunofluorescence detection of Lipocalin-2 and Myeloperoxidase positive cells in lung sections of normal sham irradiated control rats, 1, 6 and 24 hours after irradiation. Sections were stained with an antibody against Lipocalin-2 and Myeloperoxidase followed by double fluorescence immunodetection.

4.3.3 Real-time PCR analysis of total RNA from rat lung

LCN-2 gene expression was determined by RT PCR analysis for lung tissue from control and irradiated animals. Total RNA showed a not very high yet constitutive LCN-2 expression (Figure 21). LCN-2 levels in control animals were already high, and did only show up to a 9 fold increase (9 ± 2.25 -fold) within 24h after irradiation followed by a decrease. This can explain why we could not

detect any LCN-2 serum levels in lung irradiated animals by ELISA or Western blot analysis.

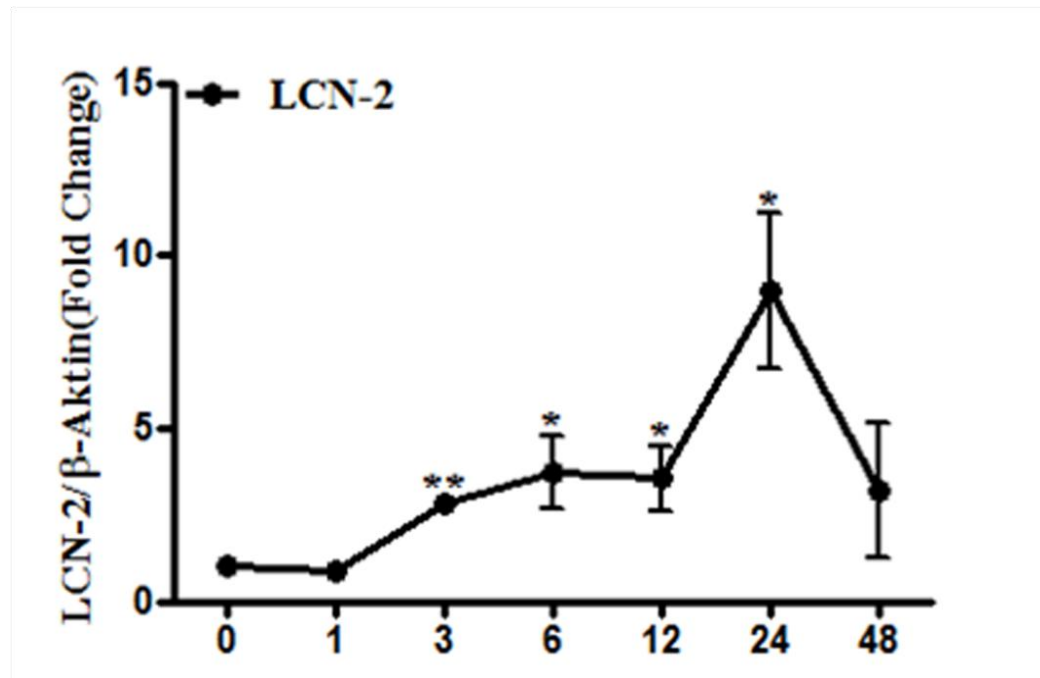


Figure 21: Fold changes of mRNA expression of Lipocalin-2 in irradiated lung tissue at time points from 1 hour to 48 hours related to normal sham irradiated control rats determined by Real Time Polymerase Chain Reaction (PCR). The results were normalized to the housekeeping gene, i.e. β -actin, fold change expression was calculated using threshold cycle (CT) values and experimental errors are shown as \pm SEM (* $p \leq 0.05$, ** $p \leq 0.005$, *** $p \leq 0.0005$ analyzed by Student's t-test, $n = 3$).

4.3.4 Real-time PCR analysis of total RNA from liver tissue of lung irradiated experiment

LCN-2 expression in upper and lower liver of the lung irradiation experiment was determined because of fact that the upper part of the liver was right below the radiation field (Figure 22). LCN-2 was expressed more in upper part of liver

than the lower not directly irradiated part. In the upper part LCN-2 expression started to increase significantly and reached a maximum up to 5 fold within 48 hours (5 ± 1.01 -fold), while the lower liver showed a significantly decreased LCN-2 expression up to 6, followed by an up-regulation at 12h only upto 1 fold (1.4 ± 0.58 -fold). LCN-2 was differently expressed in the different parts of liver which showed that irradiation cause oxidative stress and induce LCN-2 expression.

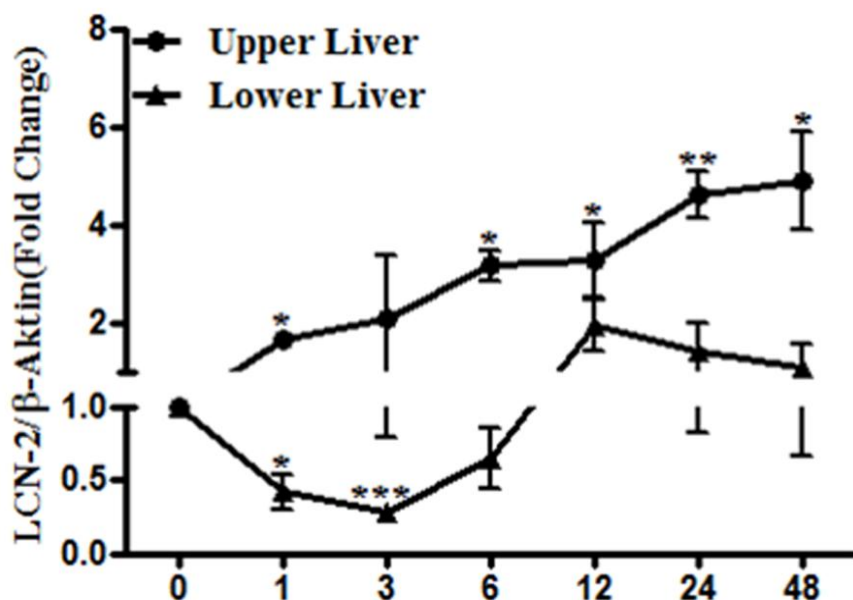


Figure 22: Fold changes of mRNA expression of LCN-2 in upper and lower liver of lung irradiated rats at different time points related to normal sham irradiated control rats determined by real time polymerase chain reaction (PCR). The results were normalized to the housekeeping gene, i.e. beta actin, fold change expression was calculated using threshold cycle (Ct) values and experimental errors are shown as \pm SEM (* $p \leq 0.05$, ** $p \leq 0.005$, *** $p \leq 0.0005$ analyzed by Student's t-test, $n = 3$).

4.3.5 Western Blot analysis of rat lung proteins

Total lung LCN-2 protein expression was analyzed by Western blot analysis. In the controls, the LCN-2 showed a strong constitutive expression and remained expressive during the course of irradiation. The irradiated lung showed a stronger protein expression of LCN-2 as compared to the liver (Figure 23). The huge LCN-2 expression confirms our immunofluorescence staining results and can explain the abundance of LCN-2 in the lung as the lung is always exposed to external environment and need extra protection.

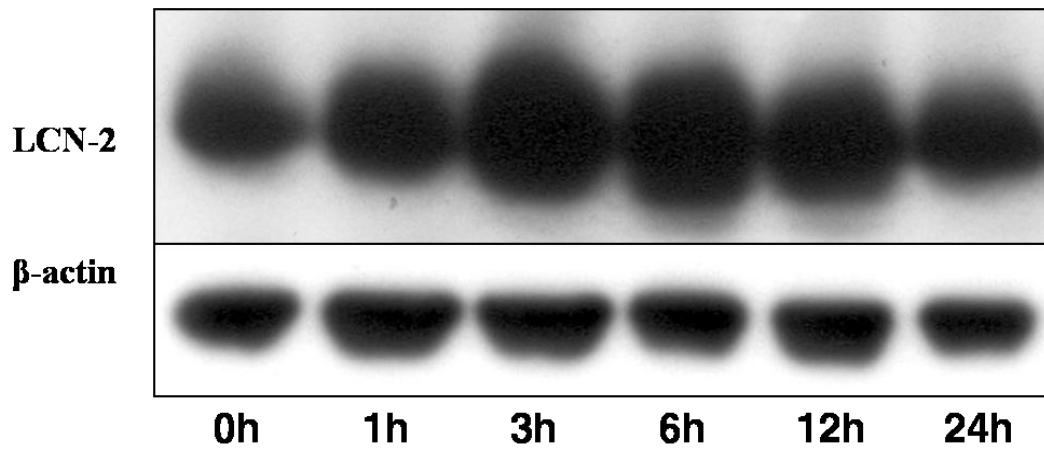


Figure 23: Western blot analysis of LCN-2 (25 kDa) from total protein of different timepoints from irradiated lung including normal sham irradiated animals. Beta actin (42 kDa) was used as loading control.

5. DISCUSSION

The present study demonstrated that LCN-2 should be fully considered as the major acute phase protein in rats and mice. In the model used of tissue injury and abscess formation induced by intramuscular injection of TO, LCN-2 gene expression in the liver showed several typical features characterizing major positive acute phase proteins. First of all, there was a dramatic increase of LCN-2 serum levels, observable after 12h from TO injection with values reaching of about 20.4 µg/ml, starting from undetectable values.

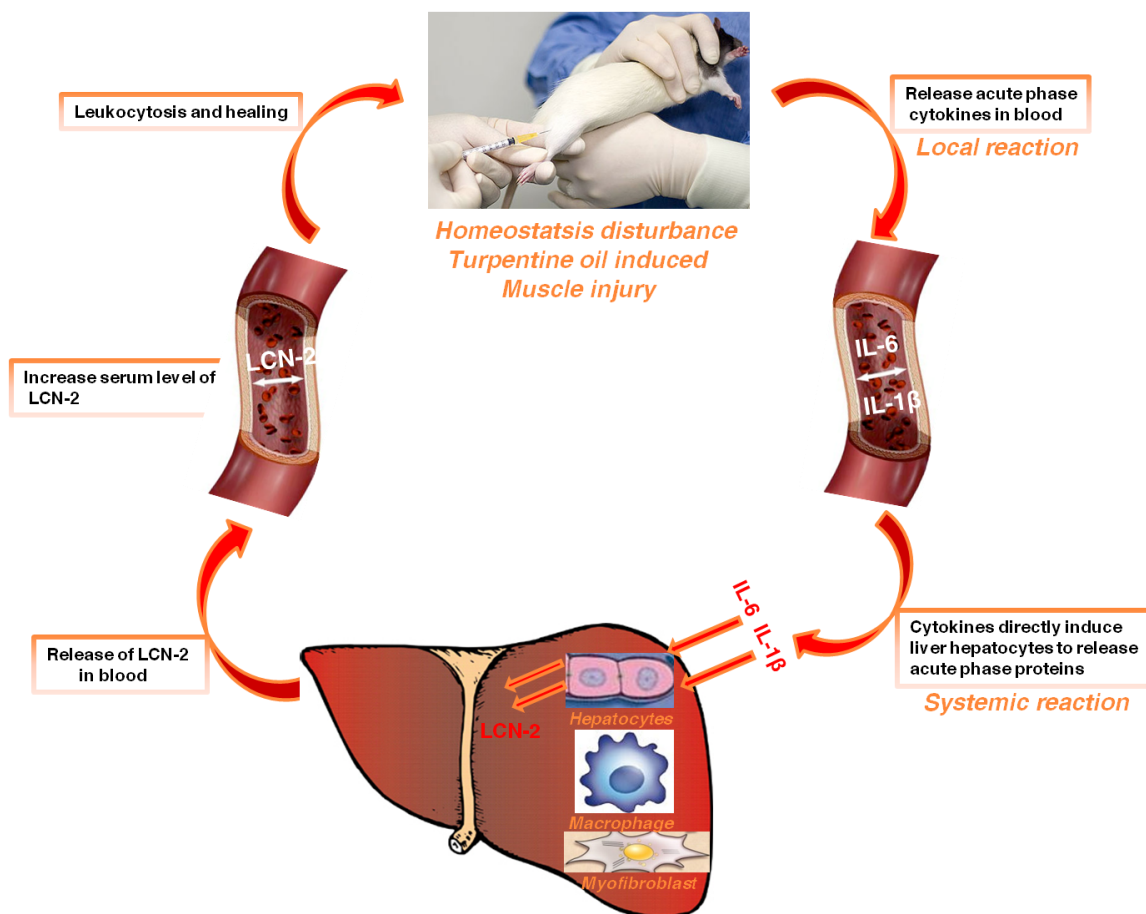


Figure 24: Homeostasis disturbance in the body causes release of different cytokines, these cytokines induce Lipocalin-2 production in liver. This Lipocalin-2 induction via the blood triggers leukocytosis and healing.

Comparing the LCN-2 gene expression pattern to α 2M (secretory protein) or to HO-1 (intracellular protein), a close similarity was found, but the order of magnitude of LCN-2 gene up-regulation was thousands-fold higher, defining LCN-2 as the major acute phase protein in the rat model of APR.

SAA is the major acute phase protein in mice and LCN-2 behaves similarly as far as magnitude and pattern of up-regulation are concerned. The changes observed in the liver at RNA level were further confirmed at the protein level. LCN-2 gene expression dramatically increased in the liver in contrast to the kidney and other organs.

In order to understand the regulation of LCN-2 under acute phase conditions, the increased production of IL-6 as shown in our previous studies with the serum level of IL-6 being much higher than IL-1 β and TNF- α (Ramadori et al., 1988;Sheikh et al., 2007), which is why we used IL-6 KO-mice for comparison with wild type mice treated with TO intramuscularly.

Comparable to what we observed in the rat liver, a strong increase of LCN-2 gene expression was detected in the liver of wild type mice, which was much lower in IL-6 ko-mice, indicating that IL-6 may actually be the main cytokine regulating LCN-2 production (Berger et al., 1997;Heinrich et al., 1990). In addition, gene expression of IL-6, IL-1 β and TNF- α was determined in TO-injured muscle, which showed a much higher expression of IL-6 compared to IL-1 β , while TNF- α showed a very low expression which was further confirmed *in vitro*.

Hepatocytes are the major liver cell type and main source of positive acute phase proteins (Kmiec, 2001). An early and significant increase of LCN-2 gene expression in IL-6-stimulated hepatocytes supports the assumption that IL-6

acts by directly interacting with the hepatocytes. α 2M and HO-1 showed low expression compared to LCN-2 in liver tissue, which further confirms *in vitro* that LCN-2 is a major acute phase protein (Table 3).

To date we know that to a lesser extent, IL-1 β stimulation determines a late increase in LCN-2 level (Cowland et al., 2003), an observation further confirmed by our experiment. In our model of acute phase response, however, IL-1 β serum levels were less than IL-6, but the role of IL-1 β cannot be ignored generally. The data support the premise that IL-6, which is strongly up-regulated in the TO-injured muscles, induces the observed changes of LCN-2 gene expression which has been shown to be inducible in different types of cells by IL-6 (Liu et al., 2003).

Liver tissue		IL-6 treated hepatocytes
	LCN-2	LCN-2
0h	27,65±0,36	0h 13,40±0,43
30min	26,57±0,35	6h 12,77±0,09
1h	27,62±0,42	12h 12,49±0,50
2h	27,32±0,53	24h 11,94±0,47
4h	23,95±0,69	
6h	19,26±0,56	
12h	15,70±0,23	
24h	15,10±0,41	
36h	14,01±0,71	
48h	15,81±0,76	

Figure 25: Difference between Cycle threshold (Ct) values of Liver tissue and IL-6 treated hepatocytes at same time points

The difference in LCN-2 expression, demonstrated in both, cycle threshold values and protein concentration between total liver homogenate and the isolated hepatocytes control group, could be ascribed to the "stress" induced by the cell isolation procedure. There was no LCN-2 expression in control liver tissue but untreated hepatocytes showed an appreciable induction of LCN-2.

In this work we also determined that neither the kidney nor the other organs are involved in LCN-2 production and the increased serum and urine levels of LCN-2 in the model of ischemia/reperfusion kidney damage (Mori et al., 2005) may have been due to the increased production in liver induced by cytokines produced in the damaged kidney.

Radiation potentially provokes activation of different genes, whose products have a protective role during an acute phase following various types of tissue damage. These products are called acute phase proteins (Magic et al., 1995). In this work, we also demonstrated that irradiation modulates Lipocalin-2 gene expression in both liver and lung but with different consequences in term of induction of changes at the serum level. In fact, the changes of serum level of Lipocalin-2 in liver-irradiated rats bear signs of an acute phase reaction (Schreiber et al., 1982).

Lipocalin-2 has been shown to take part in different cellular stress conditions and other members of the lipocalin family revealed an upregulation in situations where ROS production is high (Hemdahl et al., 2006; Lechner et al., 2001; Mishra et al., 2004; Nielsen et al., 1996; Vemula et al., 2004). The strong Lipocalin-2 induction in our model of liver and lung irradiation further confirmed that Lipocalin-2 can be strongly expressed under stress conditions.

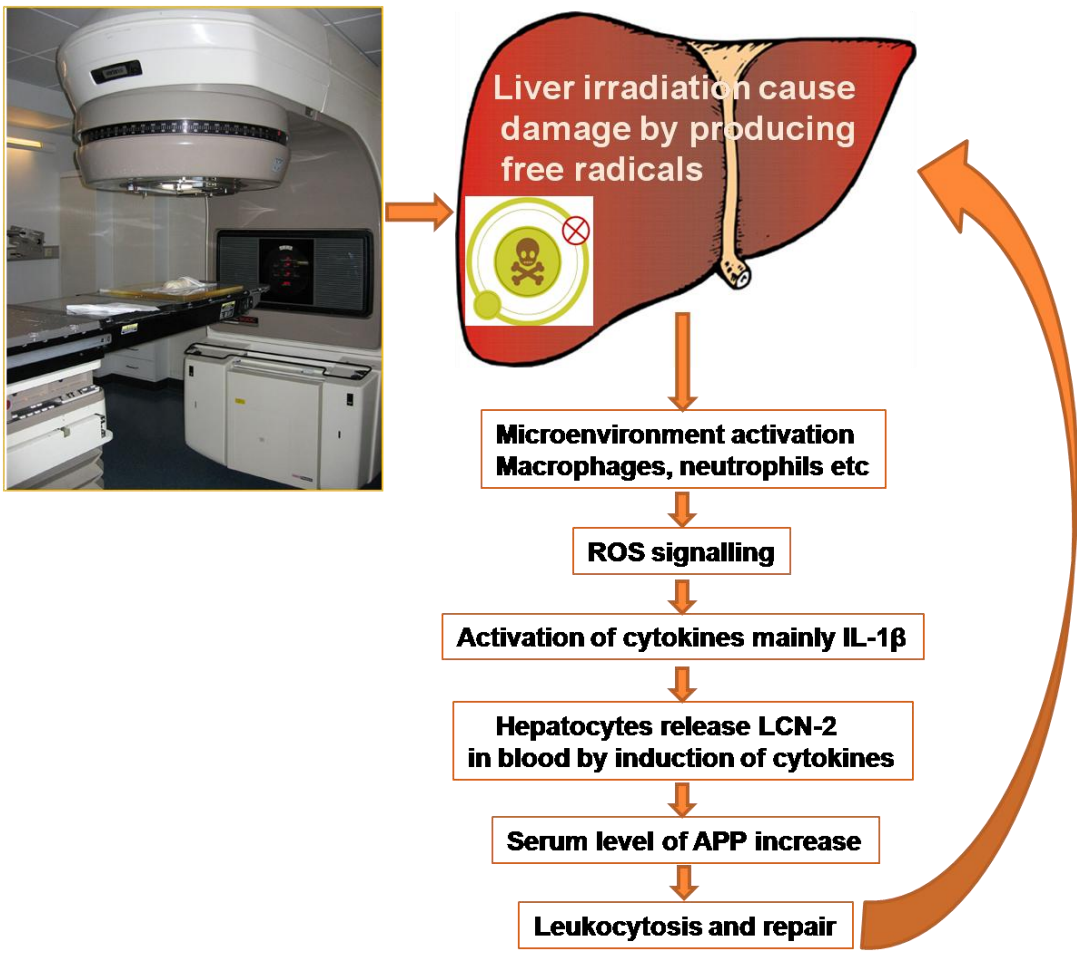


Figure 26: A pathway showing Lipocalin-2 activation, secretion and then mode of action in a damage model of liver irradiation.

Lipocalin-2 has been shown to take part in different cellular stress conditions and other members of the lipocalin family revealed an upregulation in situations where ROS production is high (Hemdahl et al., 2006; Lechner et al., 2001; Mishra et al., 2004; Nielsen et al., 1996; Vemula et al., 2004). The strong Lipocalin-2 induction in our model of liver and lung irradiation further confirmed that Lipocalin-2 can be strongly expressed under stress conditions. We confirmed our results further on protein level by Western blot analysis. Livers of irradiated rats showed the same pattern at protein level as observed at mRNA level. An increased protein expression within 1 hour after irradiation was seen

which increased every hour and reached a maximum at 24 hours. In control and irradiated lung, Lipocalin-2 was constitutively expressed at protein levels and the expression was higher as compared to mRNA level.

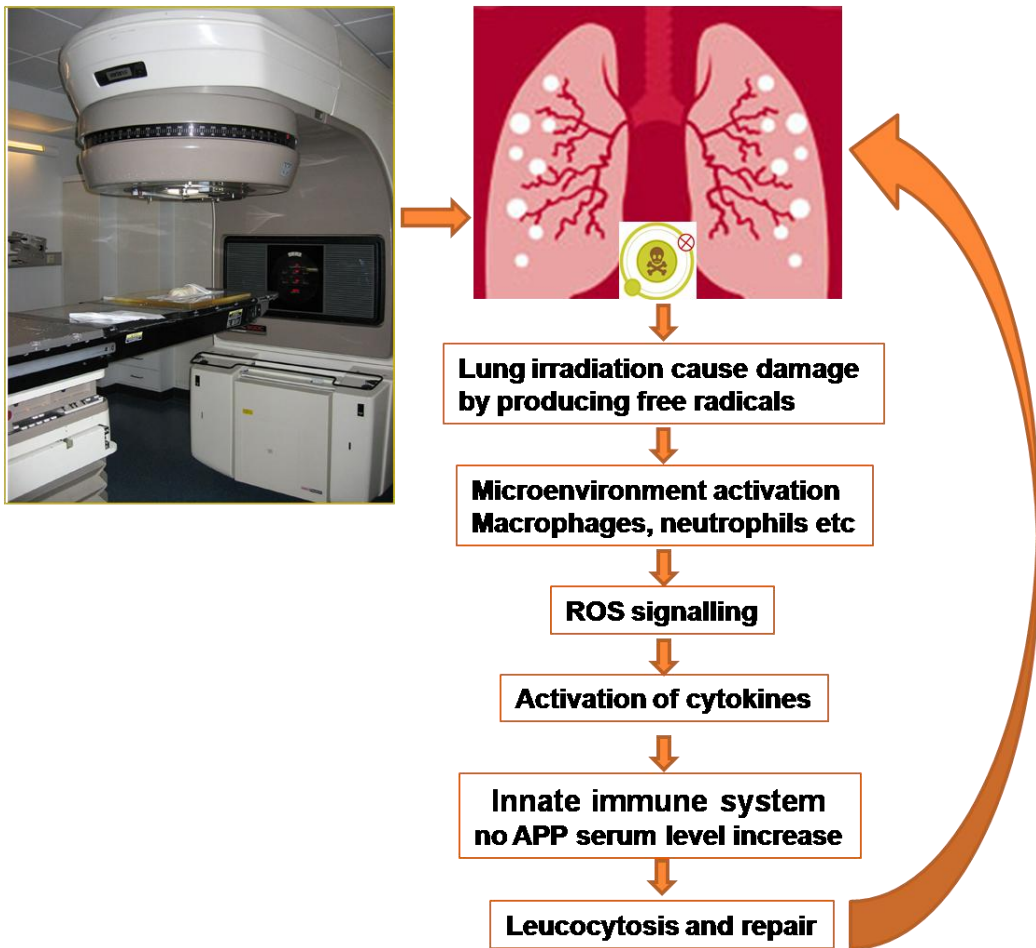


Figure 27: A pathway showing Lipocalin-2 activation, secretion and then mode of action in a damage model of lung irradiation.

The Lipocalin-2 appeared to be already present in normal lung under non-oxidative stress conditions, while in the liver it was secreted under stress conditions and only trace amounts of Lipocalin-2 were present in normal conditions. This difference of expression demonstrated that the liver is the major producer of LCN-2 under stress conditions. At the same time, a major increase

in LCN-2 was observed in blood serum level by serum ELISA and Western blot analysis in the liver, while in the lung, it was not detectable.

A volume effect has been observed for LCN-2 expression during liver and lung irradiation: Whole liver irradiation demonstrated high LCN-2 expression as compared to lung irradiation where only parts of the liver were exposed. Such a volume effect has also been observed for the development of clinical radiation-induced-liver-diseases (RILD) (Dawson et al., 2001).

This strong Lipocalin-2 induction due to hypoxia can be due to the direct action of generated free radicals in the hepatocytes (Riley, 1994) as major LCN-2 producing liver cells appeared to be the hepatocytes and not the non-parenchymal cells (Kupffer cells or myofibroblasts).

Furthermore, after irradiation neutrophil granulocytes were recruited to the liver, and were located especially around the portal and central field. However, this number does not explain the strong induction in serum levels. In contrast to the low constitutive Lipocalin-2 gene expression in control liver, expression in sham irradiated control lung was higher due to the higher number of the neutrophils within the pulmonary microcirculation (Borkham-Kamphorst et al., 2011;Hogg, 1987). However, the swap due to irradiation was not as dramatic as compared to liver. This confirms that the changes at the protein level in the serum are mostly due to changes of gene expression in the liver and much more seldom to those taking place in other organs such as the lung.

The concentration of some acute phase proteins increases early after trauma or infection suggesting their role in maintaining homeostasis and in restoring normal functions of the organism (Koj, 1985). Lipocalin-2 upregulation right after

liver irradiation denotes its role under harmful conditions whilst in the lung the role of Lipocalin-2 is relevant already under normal conditions.

The role of acute phase cytokines IL-6, IL-1 β and TNF- α seemed to be very important as they induced Lipocalin-2 expression after irradiation as was observed in model of tissue damage. IL-1 β -treated irradiated hepatocytes showed a significantly higher up-regulation compared to IL-6 and TNF- α treatment, while IL-6+TNF- α -treated irradiated hepatocytes did not enhance the effect. To date IL-1 β was considered as main acute phase cytokines changing protein profile during irradiation (Borkham-Kamphorst et al., 2011) and also IL-6, IL-17 and Lipopolysaccharides have been considered to be major inducers of Lipocalin-2 (Cowland et al., 2006; Shen et al., 2006)

In conclusion, LCN-2 can now be considered as the major positive acute-phase protein under acute phase conditions as compared to α 2M and HO-1 in rat and comparable with SAA in mouse. The liver is a main organ responsible for the production of serum LCN-2 in case of tissue damage and direct irradiation. IL-6 and IL-1 β can be the major acute phase cytokines responsible for the dramatic LCN-2 induction in different pathological conditions which cause oxidative damage such as in the acute phase model and the irradiation models described here. Lipocalin-2 is influenced by irradiation and one could suggest its protective role during irradiation and specifically, not lung, but liver single dose irradiation induces fast and detectable changes at serum level. Serum LCN-2 can be considered as a diagnostic biomarker of liver diseases but not for lung damage. Furthermore, LCN-2 may be a suitable biomarker to retrospectively analyze the irradiated liver volume in case of accidental liver irradiation to avoid RILD.

6. References

- Alpizar-Alpizar, W. et al., 2009, Neutrophil gelatinase-associated lipocalin (NGAL/Lcn2) is upregulated in gastric mucosa infected with Helicobacter pylori: Virchows Arch., v. 455, no. 3, p. 225-233.
- Amanzada, A., I. A. Malik, M. Nischwitz, S. Sultan, N. Naz, and G. Ramadori, 2011, Myeloperoxidase and elastase are only expressed by neutrophils in normal and in inflamed liver: Histochem.Cell Biol., v. 135, no. 3, p. 305-315.
- Berbeco, R. I., T. Neicu, E. Rietzel, G. T. Chen, and S. B. Jiang, 2005, A technique for respiratory-gated radiotherapy treatment verification with an EPID in cine mode: Phys.Med.Biol., v. 50, no. 16, p. 3669-3679.
- Berger, D., E. Bolke, M. Seidelmann, and H. G. Beger, 1997, Time-scale of interleukin-6, myeloid related proteins (MRP), C reactive protein (CRP), and endotoxin plasma levels during the postoperative acute phase reaction: Shock, v. 7, no. 6, p. 422-426.
- Berger, T., A. Togawa, G. S. Duncan, A. J. Elia, A. You-Ten, A. Wakeham, H. E. Fong, C. C. Cheung, and T. W. Mak, 2006, Lipocalin 2-deficient mice exhibit increased sensitivity to Escherichia coli infection but not to ischemia-reperfusion injury: Proc.Natl.Acad.Sci.U.S.A, v. 103, no. 6, p. 1834-1839.
- Borkham-Kamphorst, E., F. Drews, and R. Weiskirchen, 2011, Induction of lipocalin-2 expression in acute and chronic experimental liver injury moderated by pro-inflammatory cytokines interleukin-1beta through nuclear factor-kappaB activation: Liver Int., v. 31, no. 5, p. 656-665.

Chirgwin, J. M., A. E. Przybyla, R. J. MacDonald, and W. J. Rutter, 1979, Isolation of biologically active ribonucleic acid from sources enriched in ribonuclease: Biochemistry, v. 18, no. 24, p. 5294-5299.

Chiu, H. J. et al., 2010, Structure of the first representative of Pfam family PF09410 (DUF2006) reveals a structural signature of the calycin superfamily that suggests a role in lipid metabolism: Acta Crystallogr.Sect.F.Struct.Biol.Cryst.Commun., v. 66, no. Pt 10, p. 1153-1159.

Citrin, D., A. P. Cotrim, F. Hyodo, B. J. Baum, M. C. Krishna, and J. B. Mitchell, 2010, Radioprotectors and mitigators of radiation-induced normal tissue injury: Oncologist., v. 15, no. 4, p. 360-371.

Cowland, J. B., T. Muta, and N. Borregaard, 2006, IL-1beta-specific up-regulation of neutrophil gelatinase-associated lipocalin is controlled by IkappaB-zeta: J.Immunol., v. 176, no. 9, p. 5559-5566.

Cowland, J. B., O. E. Sorensen, M. Sehested, and N. Borregaard, 2003, Neutrophil gelatinase-associated lipocalin is up-regulated in human epithelial cells by IL-1 beta, but not by TNF-alpha: J.Immunol., v. 171, no. 12, p. 6630-6639.

Dawson, L. A., R. K. Ten Haken, and T. S. Lawrence, 2001, Partial irradiation of the liver: Semin.Radiat.Oncol., v. 11, no. 3, p. 240-246.

Devireddy, L. R., J. G. Teodoro, F. A. Richard, and M. R. Green, 2001, Induction of apoptosis by a secreted lipocalin that is transcriptionally regulated by IL-3 deprivation: Science, v. 293, no. 5531, p. 829-834.

Esmekaya, M. A., C. Ozer, and N. Seyhan, 2011, 900 MHz pulse-modulated radiofrequency radiation induces oxidative stress on heart, lung, testis and liver tissues: *Gen.Physiol Biophys.*, v. 30, no. 1, p. 84-89.

Flo, T. H., K. D. Smith, S. Sato, D. J. Rodriguez, M. A. Holmes, R. K. Strong, S. Akira, and A. Aderem, 2004, Lipocalin 2 mediates an innate immune response to bacterial infection by sequestrating iron: *Nature*, v. 432, no. 7019, p. 917-921.

Flower, D. R., 1994, The lipocalin protein family: a role in cell regulation: *FEBS Lett.*, v. 354, no. 1, p. 7-11.

Flower, D. R., 1996, The lipocalin protein family: structure and function: *Biochem.J.*, v. 318 (Pt 1), p. 1-14.

Han, W. K., and J. V. Bonventre, 2004, Biologic markers for the early detection of acute kidney injury: *Curr.Opin.Crit Care*, v. 10, no. 6, p. 476-482.

Hasegawa, M., R. Imai, K. Nojima, H. Sakurai, Y. Suzuki, M. Kawashima, M. Matsuura, Y. Nakamura, and T. Nakano, 2002, [Radiation-induced apoptosis in vivo: therapeutic significance of apoptosis in radiation therapy]: *Nihon Igaku Hoshasen Gakkai Zasshi*, v. 62, no. 10, p. 535-539.

Heinrich, P. C., J. V. Castell, and T. Andus, 1990, Interleukin-6 and the acute phase response: *Biochem.J.*, v. 265, no. 3, p. 621-636.

Hemdahl, A. L., A. Gabrielsen, C. Zhu, P. Eriksson, U. Hedin, J. Kastrup, P. Thoren, and G. K. Hansson, 2006, Expression of neutrophil gelatinase-associated lipocalin in atherosclerosis and myocardial infarction: *Arterioscler.Thromb.Vasc.Biol.*, v. 26, no. 1, p. 136-142.

HEUSTIS, A. E., and D. V. FAROWE, 1951, The hazard of radiation: Radiology, v. 57, no. 6, p. 832-836.

Hogg, J. C., 1987, Neutrophil kinetics and lung injury: Physiol Rev., v. 67, no. 4, p. 1249-1295.

Kjeldsen, L., D. F. Bainton, H. Sengelov, and N. Borregaard, 1994, Identification of neutrophil gelatinase-associated lipocalin as a novel matrix protein of specific granules in human neutrophils: Blood, v. 83, no. 3, p. 799-807.

Kmiec, Z., 2001, Cooperation of liver cells in health and disease: Adv.Anat.Embryol.Cell Biol., v. 161, p. III-151.

Koj, A., 1985, Cytokines regulating acute inflammation and synthesis of acute phase proteins: Blut, v. 51, no. 4, p. 267-274.

Kushner, I., 1993, Regulation of the acute phase response by cytokines: Perspect.Biol.Med., v. 36, no. 4, p. 611-622.

Laemmli, U. K., 1970, Cleavage of structural proteins during the assembly of the head of bacteriophage T4: Nature, v. 227, no. 5259, p. 680-685.

Le, C., V. J. Calafat, and N. Borregaard, 1997, Sorting of the specific granule protein, NGAL, during granulocytic maturation of HL-60 cells: Blood, v. 89, no. 6, p. 2113-2121.

Lechner, M., P. Wojnar, and B. Redl, 2001, Human tear lipocalin acts as an oxidative-stress-induced scavenger of potentially harmful lipid peroxidation products in a cell culture system: Biochem.J., v. 356, no. Pt 1, p. 129-135.

Liu, D. G., Q. H. Jiang, Y. Y. Wei, L. Sun, B. B. Fu, F. K. Zhao, and Q. Zhou, 2003, Gene expression profile favoring phenotypic reversion: a clue for mechanism of tumor suppression by NF-IL6 3'UTR: *Cell Res.*, v. 13, no. 6, p. 509-514.

Liu, Q., J. Ryon, and M. Nilsen-Hamilton, 1997, Uterocalin: a mouse acute phase protein expressed in the uterus around birth: *Mol.Reprod.Dev.*, v. 46, no. 4, p. 507-514.

Magic, Z., S. Matic-Ivanovic, J. Savic, and G. Poznanovic, 1995, Ionizing radiation-induced expression of the genes associated with the acute response to injury in the rat: *Radiat.Res.*, v. 143, no. 2, p. 187-193.

Malik, I. A. et al., 2010, Single-dose gamma-irradiation induces up-regulation of chemokine gene expression and recruitment of granulocytes into the portal area but not into other regions of rat hepatic tissue: *Am.J.Pathol.*, v. 176, no. 4, p. 1801-1815.

Meyer, K., J. S. Lee, P. A. Dyck, W. Q. Cao, M. S. Rao, S. S. Thorgeirsson, and J. K. Reddy, 2003, Molecular profiling of hepatocellular carcinomas developing spontaneously in acyl-CoA oxidase deficient mice: comparison with liver tumors induced in wild-type mice by a peroxisome proliferator and a genotoxic carcinogen: *Carcinogenesis*, v. 24, no. 5, p. 975-984.

Mishra, J., Q. Ma, C. Kelly, M. Mitsnefes, K. Mori, J. Barasch, and P. Devarajan, 2006, Kidney NGAL is a novel early marker of acute injury following transplantation: *Pediatr.Nephrol.*, v. 21, no. 6, p. 856-863.

Mishra, J., K. Mori, Q. Ma, C. Kelly, J. Barasch, and P. Devarajan, 2004, Neutrophil gelatinase-associated lipocalin: a novel early urinary biomarker for cisplatin nephrotoxicity: Am.J.Nephrol., v. 24, no. 3, p. 307-315.

Missiaglia, E., E. Blaveri, B. Terris, Y. H. Wang, E. Costello, J. P. Neoptolemos, T. Crnogorac-Jurcevic, and N. R. Lemoine, 2004, Analysis of gene expression in cancer cell lines identifies candidate markers for pancreatic tumorigenesis and metastasis: Int.J.Cancer, v. 112, no. 1, p. 100-112.

Mori, K. et al., 2005, Endocytic delivery of lipocalin-siderophore-iron complex rescues the kidney from ischemia-reperfusion injury: J.Clin.Invest, v. 115, no. 3, p. 610-621.

Moshage, H., 1997, Cytokines and the hepatic acute phase response: J.Pathol., v. 181, no. 3, p. 257-266.

Nielsen, B. S., N. Borregaard, J. R. Bundgaard, S. Timshel, M. Sehested, and L. Kjeldsen, 1996, Induction of NGAL synthesis in epithelial cells of human colorectal neoplasia and inflammatory bowel diseases: Gut, v. 38, no. 3, p. 414-420.

Pandey, B. N., A. Kumar, P. Tiwari, and K. P. Mishra, 2010, Radiobiological basis in management of accidental radiation exposure: Int.J.Radiat.Biol., v. 86, no. 8, p. 613-635.

Papanicolaou, D. A., R. L. Wilder, S. C. Manolagas, and G. P. Chrousos, 1998, The pathophysiologic roles of interleukin-6 in human disease: Ann.Intern.Med., v. 128, no. 2, p. 127-137.

Pepys, M. B., and G. M. Hirschfield, 2003, C-reactive protein: a critical update: J.Clin.Invest, v. 111, no. 12, p. 1805-1812.

Ramadori, G., J. D. Sipe, and H. R. Colten, 1985, Expression and regulation of the murine serum amyloid A (SAA) gene in extrahepatic sites: J.Immunol., v. 135, no. 6, p. 3645-3647.

Ramadori, G., D. J. Van, H. Rieder, and K. H. Meyer zum Buschenfelde, 1988, Interleukin 6, the third mediator of acute-phase reaction, modulates hepatic protein synthesis in human and mouse. Comparison with interleukin 1 beta and tumor necrosis factor-alpha: Eur.J.Immunol., v. 18, no. 8, p. 1259-1264.

Ramadori, P., G. Ahmad, and G. Ramadori, 2010, Cellular and molecular mechanisms regulating the hepatic erythropoietin expression during acute-phase response: a role for IL-6: Lab Invest, v. 90, no. 9, p. 1306-1324.

Riley, P. A., 1994, Free radicals in biology: oxidative stress and the effects of ionizing radiation: Int.J.Radiat.Biol., v. 65, no. 1, p. 27-33.

Sakata, K., M. Someya, Y. Matsumoto, and M. Hareyama, 2007, Ability to repair DNA double-strand breaks related to cancer susceptibility and radiosensitivity: Radiat.Med., v. 25, no. 9, p. 433-438.

Schefter, T. E., B. D. Kavanagh, R. D. Timmerman, H. R. Cardenes, A. Baron, and L. E. Gaspar, 2005, A phase I trial of stereotactic body radiation therapy (SBRT) for liver metastases: Int.J.Radiat.Oncol.Biol.Phys., v. 62, no. 5, p. 1371-1378.

Schreiber, G., G. Howlett, M. Nagashima, A. Millership, H. Martin, J. Urban, and L. Kotler, 1982, The acute phase response of plasma protein synthesis during experimental inflammation: *J.Biol.Chem.*, v. 257, no. 17, p. 10271-10277.

Seglen, P. O., 1972, Preparation of rat liver cells. I. Effect of Ca²⁺ on enzymatic dispersion of isolated, perfused liver: *Exp.Cell Res.*, v. 74, no. 2, p. 450-454.

Sheikh, N., J. Dudas, and G. Ramadori, 2007, Changes of gene expression of iron regulatory proteins during turpentine oil-induced acute-phase response in the rat: *Lab Invest*, v. 87, no. 7, p. 713-725.

Shen, F., Z. Hu, J. Goswami, and S. L. Gaffen, 2006, Identification of common transcriptional regulatory elements in interleukin-17 target genes: *J.Biol.Chem.*, v. 281, no. 34, p. 24138-24148.

Shikazono, N., C. Pearson, P. O'Neill, and J. Thacker, 2006, The roles of specific glycosylases in determining the mutagenic consequences of clustered DNA base damage: *Nucleic Acids Res.*, v. 34, no. 13, p. 3722-3730.

Sunil, V. R., K. J. Patel, M. Nilsen-Hamilton, D. E. Heck, J. D. Laskin, and D. L. Laskin, 2007, Acute endotoxemia is associated with upregulation of lipocalin 24p3/Lcn2 in lung and liver: *Exp.Mol.Pathol.*, v. 83, no. 2, p. 177-187.

Tello, K., H. Christiansen, H. Gurleyen, J. Dudas, M. Rave-Frank, C. F. Hess, G. Ramadori, and B. Saile, 2008, Irradiation leads to apoptosis of Kupffer cells by a Hsp27-dependant pathway followed by release of TNF-alpha: *Radiat.Environ.Biophys.*, v. 47, no. 3, p. 389-397.

Tron, K., R. Novosyadlyy, J. Dudas, A. Samoylenko, T. Kietzmann, and G. Ramadori, 2005, Upregulation of heme oxygenase-1 gene by turpentine oil-induced localized inflammation: involvement of interleukin-6: Lab Invest, v. 85, no. 3, p. 376-387.

Vemula, M., F. Berthiaume, A. Jayaraman, and M. L. Yarmush, 2004, Expression profiling analysis of the metabolic and inflammatory changes following burn injury in rats: Physiol Genomics, v. 18, no. 1, p. 87-98.

Viau, A. et al., 2010, Lipocalin 2 is essential for chronic kidney disease progression in mice and humans: J.Clin.Invest, v. 120, no. 11, p. 4065-4076.

Winterbourn, C. C., 2008, Reconciling the chemistry and biology of reactive oxygen species: Nat.Chem.Biol., v. 4, no. 5, p. 278-286.

Yang, J. et al., 2002, An iron delivery pathway mediated by a lipocalin: Mol.Cell, v. 10, no. 5, p. 1045-1056.

7. ACKNOWLEDGMENTS

First of all I want to thank my Allah who is most merciful and beneficent. My gratitude for him is very little in front of his countless blessings. He gave me power and enough temperament to fulfill my dreams.

Secondly I would like to thank my Professor **Dr Giuliano Ramadori** for his faith on me, for his time and encouragement which made me complete my PhD. I want to pay my gratitude to my scientific supervisors **Prof. Dr. Nils Brose** and **Dr. Michael Hoppert** for their assistance and cooperation.

I express my particular gratitude to **Dr. Nadeem Sheikh** who referred me in this department and have faith in me. My special thanks to my senior colleagues **Dr. Silke Cameron, Dr. Ihtzaz Malik, Dr Ghayyor Ahmad** and **Dr Pierluigi Ramadori** to teach me different techniques and provide me great atmosphere to work comfortably. My special thank is for **Shakil Ahmad** and **Dr Saima Zafar** for their valuable suggestions and care. I pay my regards to my colleague and friend **Naila Naz** for her time to time assistance and concern. I also like to thank other colleagues **Sajjad Khan, Gesa Martius** and **Salameh Alwashah** for their cooperation. I am thankful to the technicians of the department specially **Mrs Corinna Dunaisiki, Mrs Ranete Klages** and **Mrs Dorothea Fay** for their technical support.

I would also like to thank all my friends specially **Sara and Ibrahim Sheikh, Rose and Ibrahim Ellaik** and **Dr Saadia Zahid**, who shared the ups and downs during my stay in Germany and try to solve every problem whenever I was in trouble. I don't want to miss the opportunity to pay regard for the valuable role of my family and relatives to keep me mobile and energetic.

8. DEDICATION

To

My Father Mr Sultan Mehmood

My Mother Mrs Rukhsana Sultan

My Sister Sahar Sultan

My Brother Hasan Sultan

9. LIST OF PUBLICATIONS

1. Amanzada A, I A malik, M Nischwitz, **S Sultan**, N Naz and G Ramadori, 2011, Myeloperoxidase and elastase are only expressed by neutrophils in normal and inflamed liver: *Histochem.Cell Biol.*, v. 135, no. 3, p. 305-315.
2. **Sadaf Sultan**, Matteo Pascucci, Shakil Ahmad, Ihtzaz Ahmed Malik, Alberto Bianchi, Pierluigi Ramadori, Ghayyor Ahmad, Giuliano Ramadori, 2011, Lipocalin-2 (LCN-2) is a major acute phase protein in rat and mouse model of sterile abscess, *SHOCK accepted* (in press)
3. Wojcik M, Ramadori P, Blaschke M, **Sultan S** et al, 2011, Immunodetection of cyclooxygenase- 2 is restricted to tissue macrophages in normal rat liver and to recruited mononuclear phagocytes in liver injuy and cholangiocarcinoma. *Histochem Cell Biol.* 10.1007/s00418-011-0889-9
4. Silke Cameron; Antonia Schwartz, M.D.; **Sadaf Sultan**; Inga-Marie Schaefer, M.D.; Robert Hermann, P.D.; Margret Rave-Fräck; Clemens F. Hess, Prof.; Hans Christiansen, Prof.; Giuliano Ramadori, M.D., 2011, Radiation-induced damage in different segments of the rat intestine after external beam irradiation of the liver, Expeimental and molecular pathology, **accepted** (in press)
5. **Sultan S**, Cameron S, Ahmad S, Hielscher R, Malik IA, Schultze FC, Rave-Fräck M, Hess CF, Ramadori G, Christiansen H, Serum Lipocalin-2 is a potential Biomarker of Liver but not Lung irradiation (**submitted** in radiation radiology)

10. LIST OF ABSTRACTS

1. Pascucci M, Bianchi A, Ramadori P, **Sultan S**, Martius G, Ramadori G. IL-6 is the main mediator of Lipocalin-2 gene expression and production in a model of acute phase reaction. GASL-Conference 2011, Regensburg, Germany.
2. **Sultan S**, Schultze FC, Malik IA, Ramadori G. Expression of Lipocalin-2 (LCN-2) in rat model of TAA induced acute and chronic liver damage and CC development. EASL-Conference 2011, Bonn, Germany
3. Schultze FC, **Sultan S**, Ramadori G. Cyclooxygenase-2 expression is restricted to “resident” tissue macrophages in liver injury and cholangiocarcinoma development. EASL-Conference 2011, Bonn, Germany
4. Schultze FC, **Sultan S**, Ramadori G. Inducible cyclooxygenase-2 (COX-2) is constitutively expressed in liver tissue macrophages and can be further stimulated in isolated Kupffer cells by LPS treatment. AIO-Symposium 2011, Berlin.
5. Scultz FC, Petrova DT, **Sultan S**, Khan S, Malik IA, Naz N, Martius G, Ramadori G. Potential misidentification of cyclooxygenase-2 in liver tissue by immunohistochemistry and its prevention through specific control of antibodies. AIO-Symposium 2011, Berlin.
6. **Sultan S**, Ahmad S, Pascucci M, Ramadori G. Changes of LCN-2 gene expression in different organs in a rat model of tissue damage. Accepted for GASL-Conference 2012, Hamburg, Germany.

7. **Sultan S**, Cameron S, Ahmad S, Malik IA, Ramadori G. Serum Lipocalin-2 (LCN-2) is a potential Biomarker of Liver irradiation. Submitted for EASL-Conference 2012, Barcelona, Spain.

11. CURRICULUM VITAE (CV)

Family Name	Sultan
First name	Sadaf
Date of birth	11.09.1987
Place of birth	Lahore, Pakistan
Citizenship	Pakistani

Education

Feb. 2009-Dec. 2012: **PhD in biology**

Department of Gasteroenterologie and Endocrinology,
University Medical Center,
Georg-August University, Goettingen

Title: “Serum Lipocalin-2 (LCN-2) as a major acute phase protein under different pathological conditions: *in vivo* and *in vitro* studies”.

2006 – 2008 Degree: **Master of Science in Zoology**

University of the Punjab, Lahore, Pakistan

2004 – 2006 Degree: **Bachelors of Science**

Lahore, Pakistan

2002 – 2004 **College Education**

Lahore, Pakistan.